UNIVERSIDADE DE SÃO PAULO
FACULDADE DE ZOOTECNIA E ENGENHARIA DE ALIMENTOS

JOÃO VITOR PUTTINI PAIXÃO

The influence of ovarian follicular niche on oocyte development

Pirassununga
2023

JOÃO VITOR PUTTINI PAIXÃO

The influence of ovarian follicular niche on oocyte development

Versão Corrigida

Dissertação apresentada à Faculdade de Zootecnia e Engenharia de Alimentos da Universidade de São Paulo, como parte dos requisitos para a obtenção do título de Mestre em Ciências do programa de Pós-graduação em Biociência Animal.

Área de Concentração: Biociência Animal

Orientador: Prof. Dr. Flávio Vieira Meirelles

Pirassununga
2023

Ficha Catalográfica

Ficha catalográfica elaborada pelo
Serviço de Biblioteca e Informação, FZEA/USP, com os
dados fornecidos pelo(a) autor(a)

Paixão, João Vitor
P149i A influência do nicho folicular sobre o desenvolvimento oocitário / João Vitor Paixão ; orientador Flávio Meirelles. -- Pirassununga, 2023.
61 f.

Dissertação (Mestrado - Programa de Pós-Graduação em Biociência Animal) -- Faculdade de Zootecnia e Engenharia de Alimentos, Universidade de São Paulo.

1. Bovino. 2. Oócito . 3. Exossomos. 4. RNA-Seq. 5. GSK3B. I. Meirelles, Flávio, orient. II. Título.

CERTIFICADO

Certificamos que a proposta intitulada "A Influencia do nicho folicular sobre o desenvolvimento oocitário", protocolada sob o CEUA nº 4828131022 (ID 001957), sob a responsabilidade de **Flavio Vieira Meirelles** - que envolve a produção, manutenção e/ou utilização de animais pertencentes ao filo Chordata, subfilo Vertebrata (exceto o homem), para fins de pesquisa científica ou ensino - está de acordo com os preceitos da Lei 11.794 de 8 de outubro de 2008, com o Decreto 6.899 de 15 de julho de 2009, bem como com as normas editadas pelo Conselho Nacional de Controle da Experimentação Animal (CONCEA), e foi **APROVADA** pela Comissão de Ética no Uso de Animais da Faculdade de Zootecnia e Engenharia de Alimentos da Universidade de São Paulo - FZEA/USP (CEUA/FZEA) na reunião de 22/11/2022.

We certify that the proposal "The influence of the ovarian folicular niche on the oocyte development", utilizing 100 Bovines (100 females), protocol number CEUA 4828131022 (ID 001957), under the responsibility of **Flavio Vieira Meirelles** - which involves the production, maintenance and/or use of animals belonging to the phylum Chordata, subphylum Vertebrata (except human beings), for scientific research purposes or teaching - is in accordance with Law 11.794 of October 8, 2008, Decree 6899 of July 15, 2009, as well as with the rules issued by the National Council for Control of Animal Experimentation (CONCEA), and was **APPROVED** by the Ethic Committee on Animal Use of the School of Animal Science and Food Engineering - (São Paulo University) (CEUA/FZEA) in the meeting of 11/22/2022.

Finalidade da Proposta: Pesquisa (Acadêmica)

Vigência da Proposta: de 09/2022 a 03/2023 Área: Biociência Animal

Origem:	Prefeitura do Campus USP Fernando Costa			
Espécie:	Bovinos	sexo: Fêmeas	idade: 24 a 128 meses	Quantidade: 100
Linhagem:	SRD		Peso: 380 a 900 kg	

Pirassununga, 29 de novembro de 2022

Profa. Dra. Luciane Silva Martello
Presidente da Comissão de Ética no Uso de Animais
Faculdade de Zootecnia e Engenharia de Alimentos da Universidade de São Paulo - FZEA/USP

Profa. Dra. Fabiana Fernandes Bressan
Vice-Presidente da Comissão de Ética no Uso de Animais
Faculdade de Zootecnia e Engenharia de Alimentos da Universidade de São Paulo - FZEA/USP

FOLHA DE APROVAÇÃO

Nome: João Vitor Puttini Paixão

Título: A influência do nicho folicular sobre o desenvolvimento oocitário

Tese apresentada à Faculdade de Zootecnia e Engenharia de Alimentos da Universidade de São Paulo, como parte dos requisitos para a obtenção do título de Mestre em Ciências do programa de Pós-graduação em Biociência Animal.

Área de Concentração: Reprodução Animal

Data:_____/_____/_____

BANCA EXAMINADORA

Prof.

Dr._____

Instituição:_____Julgamento:_____

Prof.

Dr._____

Instituição:_____Julgamento:_____

Prof.

Dr._____

Instituição:_____Julgamento:_____

Prof.

Dr._____

Instituição:_____Julgamento:_____

Dedico este trabalho...

Aos meus pais, ***Maria Regina*** *e* ***Luis Eduardo****, meus primeiros mestres, com amor e carinho sempre me incentivaram a estudar e trabalhar duro para alcançar meus objetivos.*

Aos meus irmãos ***Pedro Henrique*** *e* ***Daniel Luis****, meus grandes companheiros, para sempre grato pela nossa cumplicidade!*

Vocês foram...são...e sempre serão meu porto seguro! Amo vocês para sempre!

AGRADECIMENTOS

Gostaria de agradecer primeiramente a meu orientador **Prof. Dr. Flávio Meirelles** por essa grande oportunidade que o senhor me concedeu de fazer parte da equipe do LMMD e me orientar durante todos esses anos. Sou imensamente grato por sempre confiar em mim, pelo imenso aprendizado que tive com o senhor, pela paciência, atenção, vasto conhecimento e ótimas conversas na hora do café! Serei sempre muito grato por tudo isso professor! Também gostaria de fazer um agradecimento especial ao **Prof. Dr. Juliano Da Silveira, Dra. Gabriella Mamede Andrade** e ao **Dr. Ricardo Nociti** por contribuírem imensamente com os dados deste trabalho.

Agradeço pela apoio e conhecimento dos professores doutores **Felipe Perecin** e **Lawrence Smith** que juntamente com a contribuição das professoras doutoras **Claudia Verde Leal, Fabiana Bressan** e a nossa grande especialista do laboratório **Dra. Cibele Prado** engrandeceram este trabalho.

Sou imensamente grato aos meus **amigos/companheiros de laboratório**: **Strepa, Ju Sangalli, Jéssica, Amanda, Japa, Naomi, Deba, Ramon, Léo, Ale, Nat, Kai, Paola, Giu, Gis, Fer, Ma, Maíra, Ju Ferst, Fran, Lu, Helena, Matheus, Lais, estagiários/ICs** e **demais companheiros da pós-graduação!** Obrigado pelo apoio no dia-a-dia, troca de conhecimentos, risadas e boas conversas!

Aos meus amigos próximos **PCR, Sorteio, Ian, Gabriel e Fotossíntese** foram meus grandes companheiros nesses tempos do mestrado, sempre prontos para me ajudar quando precisava e também para nos divertirmos juntos. Também gostaria de agradecer a todos os meus amigos da **República Tatu Currido** que me acompanharam nesses anos e sempre achavam uma hora boa para descontração, conselhos e boas conversas.

Agradeço à **USP** e a **FZEA** por me acolherem durante todos esses anos, por toda estrutura para a realização deste trabalho e pela sua equipe de colaboradores e técnicos.

À **Dra. Julianne Vargas** do **Hemocentro** da **FMRP-USP** pela grande ajuda com as imagens do microscópio confocal. À **CAPES*** pela concessão da bolsa de mestrado, bolsa **PAE** auxílios, e a **FAPESP** pelo suporte financeiro em equipamentos e insumos para realização deste trabalho.

Por fim, mas não menos importante, queria fazer um agradecimento especial aos **todos meus familiares** que mesmo de longe sempre me apoiaram imensamente nessa jornada do mestrado. Sou imensamente grato a vocês!

Muito obrigado todos!

*O presente trabalho foi realizado com apoio da Coordenação de Aperfeiçoamento de Pessoal de Nível Superior – Brasil (CAPES) – Código de Financiamento 001

* This study was financed in part by the Coordenação de Aperfeiçoamento de Pessoal de Nível Superior - Brasil (CAPES) - Finance Code 001

"As maiores descobertas muitas vezes não residem em encontrar coisas novas, mas em ver coisas familiares de novas maneiras." (Alexander Fleming)

RESUMO

Paixão, J.V. P**. A influência do nicho folicular sobre o desenvolvimento oocitário**. 61 f. Dissertação – Faculdade de Zootecnia e Engenharia de Alimentos, Universidade de São Paulo, Pirassununga, 2023.

Os exossomos (Exos), vesículas extracelulares pequenas, presentes no fluido folicular (FF), atuam na comunicação intercelular, transportando conteúdos bioativos, como mRNAs e lnc-RNAs, contribuindo para a maturação do ovócito. Assim sendo, especula-se que Exos presentes no fluido de folículos contendo oócitos de boa qualidade ou má qualidade são distintos no seu conteúdo de RNA. O primeiro objetivo deste trabalho foi compreender, detalhadamente, a relação entre o contéudo de RNAs poli-adenilados de Exos oriundos do FF, e o desenvolvimento oocitário e embrionário. Para tanto, Exos do FF foram coletados e isolados de folículos com diâmetro de 3 a 6 mm, utilizando um modelo retrospectivo bovino previamente descrito. Para rastrear sua competência, o FF e o ovócito foram recuperados individualmente através da dissecção de folículos oriundos ovários, selecionados aleatoriamente, de abatedouros. Os gametas foram maturados, ativados partenogeneticamente e cultivados individualmente por 7 dias. Com base nos registros de desenvolvimento, os ovócitos e seus respectivos fluidos foliculares foram classificados e separados em três grupos, de acordo com a competência de desenvolvimento: Grupo NCLEAV (Incompetente Maduro): Ovócitos maduros *in vitro* que não se dividiram após a ativação partenogenética; Grupo CLEAV (Incompetente Clivado): Ovócitos que se dividiram após a ativação, mas bloquearam o desenvolvimento no 3º ou 4º ciclo celular; Grupo BLAST (Blastocistos): oócitos que se desenvolveram até o estágio de blastocisto. Foram realizadas análises de expressão gênica diferencial, genes exclusivos e genes centrais a partir dos dados transcriptômicos, e diferenças transcricionais entre os grupos mais competentes (BLAST) e menos competentes (CLEAV e NCLEAV) (p-ajust.<0.1) foram observadas. Interessantemente, vários transcritos gênicos encontrados significativamente alterados entre esses grupos estavam relacionados a vias de sinalização associadas à proliferação celular e modulação da meiose, como as vias de sinalização WNT, PI3K-Akt e Hippo. Devido à sua função fundamental em todas essas vias, a GSK3 (Glicogênio Sintase Quinase 3) foi selecionada como proteína candidata que potencialmente regula essas vias de sinalização e a competência do ovócito. Para testar isso, os ovócitos foram maturados sob três condições: 1) CTL (controle); 2) Tratamento com

DKK1, que estimula indiretamente a GSK3β através da inibição da via de sinalização WNT pelo DKK-1 (proteína relacionada ao Dickkopf 1); 3) Tratamento com CHIR, que inibe diretamente a GSK3β através da sonda química CHIR99021. Foram observadas taxas de extrusão de corpúsculo polar, e os ovócitos maduros foram ativados partenogeneticamente e cultivados *in vitro*. O grupo CHIR apresentou uma maior taxa de maturação em comparação com as outras, mas não foram observadas diferenças na clivagem e no desenvolvimento a blastocisto. Para melhor compreender o efeito de inibição, a β-catenina foi localizada por imunocitoquímica, e uma maior localização nuclear foi observada novamente no grupo CHIR. Em conclusão, o modelo retrospectivo identificou genes e vias presentes em Exos derivados de FF que estão associadas à competência do oócito. A modulação da GSK3β nos COCs aumentou a taxa de extrusão do 1º corpúsculo polar enquanto as demais taxas não apresentaram alterações estatísticas. Contudo, as características da modificação induzida pela inibição da GSK3β foram semelhantes às observadas *in vivo* em ovócitos humanos.

Palavras-chave: Bovino; Oócito; Exossomos; RNA-Seq; GSK3β.

ABSTRACT

Paixão, J.V. P. **The influence of ovarian follicular niche on oocyte development.** 61 f. Master's Thesis – Faculdade de Zootecnia e Engenharia de Alimentos, Universidade de São Paulo, Pirassununga, 2023.

Exosomes (Exos), small extracellular vesicles, present in follicular fluid (FF), act in intercellular communication, carrying bioactive contents, such as mRNAs and lnc-RNAs, contributing to oocyte maturation. Hence, it is speculated that Exos present in the fluid of follicles containing good quality or poor quality oocytes are different in their RNA content. The first aim of this work was to comprehend, in detail, the relation between the content of polyadenylated RNAs of Exos originating from the FF and the oocyte/embryo development. To this end, the Exos from the FF were collected and isolated from 3 to 6 mm diameter follicles using a retrospective bovine model previously described. To track its competence, FF and oocyte were individually recovered through the dissection of follicles from randomly selected slaughterhouse`s ovaries. Gametes were matured, parthenogenetically activated and cultured individually for 7 days. Based on developmental records, oocytes and their respective follicular fluids were classified and separated in three groups, accordingly to developmental competence: NCLEAV Group (Incompetent Mature): Oocytes matured *in vitro* that did not cleave after parthenogenetic activation; CLEAV Group (Incompetent Cleaved): Oocytes cleaved after parthenogenetic activation that blocked the development at 3rd or 4th cell cycle; BLAST Group (Blastocysts): Oocytes that developed to the blastocyst stage. Differential gene expression, exclusive and HUB genes analyses of the transcriptomic data were performed, and transcriptional differences among the more competent (BLAST) and less competent (CLEAV and NCLEAV) groups (p-adjust.<0.1) were observed. Interestingly, several gene transcripts found significantly altered among these groups were related to signaling pathways associated with cell proliferation and meiosis modulation such as WNT, PI3K-Akt and Hippo signaling pathways. Due to its key function in all pathways, GSK3 (Glycogen Synthase Kinase 3) was selected as a candidate protein that potentially regulates these signaling pathways and the oocyte competence. To test this, oocytes were matured under 3 conditions: 1) CTL (control); 2) DKK1 treatment that indirectly stimulates GSK3β through DKK-1 (Dickkopf related protein 1) inhibition of the WNT signaling pathway; 3) CHIR treatment that directly inhibits GSK3β through the chemical probe CHIR99021. Polar body extrusion rates were observed, mature oocytes were parthenogenetically activated and *in vitro* cultured. The CHIR group presented a

higher maturation rate compared with the others but no differences were observed in cleavage and Blastocyst development. To further understand the inhibition effect β-catenin was localized by immunocytochemistry and a increased nuclear localization was observed in CHIR group again. In conclusion the retrospective model identified crucial genes and pathways present in FF-derived Exos that are associated with oocyte competence. Modulation of GSK3β in COCs increased the extrusion rate of the 1st polar body while the other rates did not show statistical changes. However, the characteristics of the modification induced by GSK3β inhibition were similar to those observed *in vivo* in human oocytes.

Key-words: Bovine; Oocyte; Exosomes; RNA-Seq; GSK3B.

CONTENT

1. GENERAL INTRODUCTION

One of the main aspects of oocyte quality is the ability, or potential, of an oocyte to reach maturity, be fertilized, develop into a blastocyst and ultimately generate and maintain a pregnancy, these characteristics are known as oocyte competence. (LONERGAN et al., 2003; SIRARD et al., 2003, 2006). The process of acquiring oocyte competence is a progressive transformation that involves adequate nuclear and cytoplasmic maturation. Nuclear maturation is marked mainly by the condensation and segregation of chromosomes, while cytoplasmic maturation is characterized by the accumulation of RNAs, proteins, metabolites and redistribution of organelles. Both are influenced by the interaction of the oocyte with external factors and the follicular microenvironment during folliculogenesis. (KRISHER, 2013; READER; STANTON; JUENGEL, 2017; SIRARD, 2019; WALKER; BIASE, 2020).

Folliculogenesis is the process of formation, growth and maturation of ovarian follicles, the structural and functional unit of mammalian ovaries responsible for hormone production and oocyte development (COMBELLES et al., 2010; LEITÃO et al., 2009; PALMA et al., 2012). Its development starts from primordial germ cells during fetal life and ends at ovulation. More precisely, between the prophase I and metaphase II (MII) of the oocyte, creating in this period an essential microenvironment for the growth, capacitation and maturation processes of the oocyte, that is, oogenesis (AERTS; BOLS, 2010; HENNET; COMBELLES, 2012; MOTA, 2008).

During folliculogenesis, follicles are classified according to their degree of evolution: pre-antral (primordial, primary and secondary) and antral (tertiary and pre-ovulatory), due to the absence or presence, respectively, of the antrum, an area filled by follicular fluid (FF) (AERTS; BOLS, 2010). Such fluid, present in antral ovarian follicles, is formed from the plasma and cellular secretions of the granulosa and theca within the follicle. (FORTUNE, 1994). Follicular cells have a considerable influence on FF concentrations, as they secrete a

variety of molecules that include proteins and growth factors, which have effects on the oocyte, in the regulation and resumption of meiosis. (HENNET; COMBELLES, 2012). Taking into account the relevance of the interactions between the oocyte and the follicular niche, it is possible to state that alterations in the FF composition are associated with the oocyte quality of cattle and humans. Several studies indicate that FF metabolites and hormones are related to oocyte competence and may influence fertility (DA SILVEIRA et al., 2021; MATOBA et al., 2014; O'BRIEN; WINGFIELD; O'SHEA, 2019). Therefore, the analysis of the follicular niche proves to be a coherent step in the development of non-invasive methods for the selection of oocytes and embryos. As FF is a routine by-product of oocyte retrieval, it is the ideal sample for such an analysis.

Present in FF, there are extracellular vesicles (EVs), that comprise exosomes (50±150 nm) and microvesicles (100±1000 nm). EVs are a heterogeneous group of small, spherical, membrane-bound biological structures known to be secreted by nearly every known cell type. Their basic structure formed by a lipid bilayer makes them a safe way to transport molecules compared to free molecules in fluids. (GODAKUMARA et al., 2021; SKOG et al., 2008; TAYLOR; GERCEL-TAYLOR, 2008). In the interaction between cumulus cells and the oocyte, in addition to the paracrine pathway, an essential part of this interaction is mediated by transzonal projections (TZPs). These projections originate from the cumulus cells and penetrate the zona pellucida, reaching the oocyte to transfer, through GAP junctions, small molecules essential for the homeostatic regulation of the oocyte and also through a mechanism called gametic synapse that secretes and incorporates RNAs through EVs (ALBERTINI et al., 2001; MACAULAY et al., 2014, 2016). Thus, EVs carry transcriptomic contents for intercellular communication, such as microRNAs (miRNAs) and mRNA, among others, during follicular development in horses, cattle and humans (DA SILVEIRA et al., 2012; O'BRIEN et al., 2020; VALADI et al., 2007). Furthermore, the supplementation of EVs from 3 to 6 mm diameter

follicles during IVM and IVC is capable of altering the global pattern of methylation and hydroxymethylation of DNA in bovine embryos produced *in vitro* (DA SILVEIRA et al., 2017).With the identification of biomarkers such as EVs, it becomes possible to standardize a non-invasive method of assessing oocyte quality (SANTOS et al., 2018; WALLACE et al., 2012).

Recently, it was demonstrated in cattle that the miRNAs present in small EVs, similar to exosomes, are important in the acquisition of oocyte competence and in embryonic development, as they are endocytosed by the oocyte cumulus complex during IVM (DE ÁVILA et al., 2019). Moreover, in a retrospective study based on transcriptomic data from bovine FF, the phosphatidylinositol-3-kinase/protein kinase B (PI3K-Akt) signaling pathway, crucial for follicular development, was differentially regulated and has the potential to lead to oocyte competence (ANDRADE et al., 2017; GROSBOIS; DEMEESTERE, 2018; MAKKER; GOEL; MAHDI, 2014). However, the transcriptomic analysis performed using RT-PCR and RNA sequencing techniques in previous studies, in cattle, focused only on the profile of miRNAs, not covering the mRNAs and lnc-RNAs also present in exosomes and their possible associations with pathways related to oocyte development (HUNG et al., 2017; NAVAKANITWORAKUL et al., 2016).

Exosomal mRNAs and lncRNAs, play a vital role in oocyte development and follicular microenvironment. Recent studies have detected several mRNAs and lnc-RNAs from FF-derived exosomes associated with PI3K-Akt and other signaling pathways related to oocyte development, such as MAPK and Hippo (MATSUNO et al., 2019; WANG et al., 2021). Nonetheless, the association between these mRNAs and lncRNAs profiles and the oocyte competence in bovines remain imprecise, highlighting the need for further research in this area.

2. CHAPTER 1: ARTICLE - Characterization of poly-A tail RNAs present in small extracellular vesicles of follicles containing oocytes with different developmental competence

Abstract

To further understand of the role of exosomes in the acquisition of developmental competence, we compared the mRNA content of exosomes from the fluid of follicles containing oocytes that were able develop to the blastocyst stage to those that arrest at earlier stages of development. Our results show the main alterations observed between the transcriptomic profiles of the more competent (BLAST) and less competent (CLEAV and NCLEAV) groups ($q<0.1$). In this article we highlighted the accumulation of transcripts from relevant proteins linked to signaling pathways previously identified in our group studies such as PI3K-Akt, Hippo and Wnt. Moreover, GSK3β (Glycogen Synthase Kinase 3 β) activity in the high quality follicular niche (BLAST) appeared to play key role between the PI3K-Akt and Wnt pathways. To evaluate this, oocytes were matured under 3 conditions: 1) CTL (control); 2) DKK1 treatment that indirectly stimulates GSK3β through DKK-1 (Dickkopf related protein 1) inhibition of the WNT signaling pathway; 3) CHIR treatment that directly inhibits GSK3β through the chemical probe CHIR99021. Polar body extrusion rates were observed, mature oocytes were parthenogenetically activated and in vitro cultured. The GKS3β modulation presented only effect on COCs of the CHIR group, increasing the first polar body extrusion rates. Furthermore, the inhibition effect β-catenin localized by immunocytochemistry and a increased nuclear localization was observed in CHIR group again. Concluding, the retrospective model identified crucial genes and pathways present in FF-derived Exos that are associated with oocyte competence. However, the modification induced by GSK3β inhibition were similar to those observed in vivo in human oocytes.Since the treatment interfered in β-catenin localization in the cumulus cells it is tempting to speculate that the treatment resulted increased dysmature gametes rates. Furthers studies are needed to confirm this speculation.

2.1. INTRODUCTION

Metabolites and hormones from both human and bovine follicular fluids have been shown to be related to oocyte competence and influence fertility (ANDRADE et al., 2017; MATOBA et al., 2014; O'BRIEN; WINGFIELD; O'SHEA, 2019). Using biomarkers in follicular extracellular compartments, such as extracellular vesicles (EVs), it has become possible to standardize a non-invasive method of estimating oocyte quality (SANTOS et al., 2018; WALLACE et al., 2012). In this context, the analysis of the follicular niche by measurements of the components of the follicular fluid, a routine by-product in oocyte retrieval, is a coherent strategy in the development of non-invasive methods to study oocytes that contain the necessary requisites for the production of a viable embryo.

Exosomes (Exos), small EVs (50 to 150 nm) found in the follicular fluid and have been shown to carry numerous bioactive molecules for intercellular communication, including microRNAs (miRNAs), long non-coding RNAs (lncRNAs), messenger RNAs (mRNAs) (GODAKUMARA et al., 2021; SKOG et al., 2008; TAYLOR; GERCEL-TAYLOR, 2008). Relevant reproductive functions of exosome-like vesicles has been described in several mammalian species (MACHTINGER; BACCARELLI; WU, 2021) and, in bovine follicular fluid (bFF), have been shown to play main roles during oocyte maturation and competence acquisition processes (DA SILVEIRA et al., 2017; RODRIGUES et al., 2019; UZBEKOVA et al., 2020).

Recently, analysis of bFF has demonstrated that the miRNAs present in EVs are endocytosed by the cumulus-oocyte complex during *in vitro* maturation (IVM) and, thus, could be involved in the acquisition of oocyte competence. Moreover, mRNAs and lncRNAs have been detected in Exos derived from porcine and human follicular fluids and could be improving oocyte quality (MATSUNO et al., 2019; WANG et al., 2021). However, transcriptomic analysis performed using the RNA sequencing (RNA-Seq) techniques have focused

exclusively on the miRNA profile, while the mRNA profile present in EVs and their possible association with pathways related to oocyte competence remain lacking. Furthermore, previous retrospective studies using bovine follicular components have validated by granulosa cells (GCs) proteomics and Exos lipidomics that several key cellular pathways were differentially regulated with regard to oocyte competence (ANDRADE et al., 2017; DA SILVEIRA et al., 2021). Therefore, we hypothesize that the polyadenylated RNA profiles of Exos from follicular fluids containing good quality oocytes differ from those containing poor quality oocytes. We used a retrospective model in which individual ovarian follicles were dissected to recover both the FF for assessment by RNA-seq of transcripts present in the Exos and the counterpart oocyte for assessing its developmental competence to undergo cleavage and development to the blastocyst stage after parthenogenetic activation. Our overall goal is to understand in detail the effect of the follicular microenvironment on the oocyte and embryonic development and offer subsidies for improvements in the *in vitro* production process of bovine embryos and other mammalian species. Then, to test the effectiveness of the retrospective RNA-Seq analysis we interfered with the GSK3β enzyme/pathway due to its central role in the Wnt and PI3K-Akt signaling pathways.

2.1. MATERIAL AND METHODS

The procedures described and reported here did not involve the use of live animals. All tissues were recovered *post mortem*. This article was approved by the Ethics Committee of the Faculty of Animal Science and Food Engineering of the University of São Paulo under protocol number 14.1.688.4.1. All the experiments were conducted in accordance with the International Guiding Principles for Biomedical Research Involving Animals (Society for the Study of Reproduction). The reagents and culture media used were purchased from the Sigma-Aldrich company (St. Louis, MO, USA), when this is not the case, the origin will be mentioned.

Bovine ovaries (mixed breed cows, randomly selected, independently of their estral cycle) were collected at a commercial slaughterhouse in the region of Pirassununga – SP and transported in thermos bottles with pre-warmed sterile saline solution (0.9% NaCl), at a temperature of approximately 37 °C, within an interval of up to 3 h after slaughter.

2.1.1. Sample collection and in vitro embryo production for retrospective analysis

Four ovaries per routine were randomly chosen and five follicles (ranging from 3 to 6 mm) were individually dissected. In order to collect the contents, dissected follicles were ruptured individually using 18G needles under the stereomicroscope. The follicular fluid samples were collected in 0.6 mL microtubes and the *cumulus* oocyte complexes (COCs) were isolated for the *in vitro* production of parthenogenetic embryos. Detailed maturation, parthenogenetic activation and embryo culture procedures were previously described by Da Silveira et al. (DA SILVEIRA et al., 2021). Briefly, COCs were matured individually in 9 µL droplets of *in vitro* maturation medium (TCM-199) buffered with bicarbonate and supplemented with 10% FCS, 0.2 mM sodium pyruvate, 50 mg/mL of follicle stimulating hormone (FSH) (Folltropin-V, Bioniche Animal Health Belleville, Canada) and 50 mg/mL hCG (Vetcore®, Hertape Calier), under mineral oil at 38.5 C incubator and 5% CO2 in air atmosphere. After 19 h of individual *in vitro* maturation (IVM), COCs were individually denuded by fine-pipetting and returned to maturation medium and incubator until the activation protocol. Oocytes were classified into matured (IVM +) or non-matured (IVM -) based on the presence or absence of the first polar body (1^{st} PB), respectively. After 26 h of maturation, all oocytes were parthenogenetically activated, regardless of presence or not of a 1^{st} PB. Oocytes were washed three times with H199 medium (TCM-199 with 25 mM HEPES) containing 0.5 mg/mL bovine serum albumin (BSA), 0.2 mM pyruvate, and 50 µg/mL gentamicin. After

washing, oocytes were activated, using the same medium supplemented with 5mM ionomycin for 5 min. Then, the oocytes were washed thrice with H199 saturated media (TCM-199 with 25mM Hepes containing 30 mg/mL BSA, 0.2 mM pyruvate, and 10 μg/mL gentamicin) and washed thrice right away with synthetic oviduct fluid (SOF) supplemented with 5 mg/mL BSA, 2.5% extracellular vesicles depleted-fetal calf serum (EVsfree-FCS), 0.2 mM pyruvate, 10 mg/mL gentamicin, and 2mM 6-dimethylaminopurine (6-DMAP). Finally, the oocytes were transferred into 9 μL single droplets of DMAP-supplemented SOF and incubated at 38.5 ºC with 5% CO_2 in air for 3 h.

Following Ionomycin-DMAP parthenogenetic activation, oocytes were washed three times with SOF medium supplemented with 5 mg/mL BSA, 2.5% EVs free-FCS, 0.2 mM pyruvate, and 10 μg/mL gentamicin, and subsequently co-cultured with a monolayer of cumulus cells on the same plate in 9 μL droplets of fresh culture medium covered with mineral oil at 38.5 ºC in a humid atmosphere of 5% O_2, 5% CO_2 and 90% N_2 for 8 days. The presumptive embryos were evaluated for cleavage at D3 (48 h) and for blastocyst development at D7 (168 h) post-activation. More details about the development rates were described elsewhere (ANDRADE et al., 2017).

2.1.2. Retrospective Analysis

From these routines, three groups were formed according to the stage at which the embryos stopped their development: noncleaved (NCLEAV - presumptive zygotes, derived from mature and non-mature oocytes were unable to cleave by D3 after parthenogenetic activation), cleaved (CLEAV - parthenogenetic embryos that cleaved, but stopped their development before reaching the blastocyst stage by D7) and blastocysts (BLAST - parthenogenetic embryos that developed to the blastocyst stage. Following the retrospective

assessment of oocytes competence, respective individual FFs were identified as NCLEAV (n=3), CLEAV (n=3) and BLAST (n=3) and pooled. Each pool was composed by five individual bFF samples (10-110µL, approximately) from which the Exos were isolated for subsequent analysis (Figure 1).

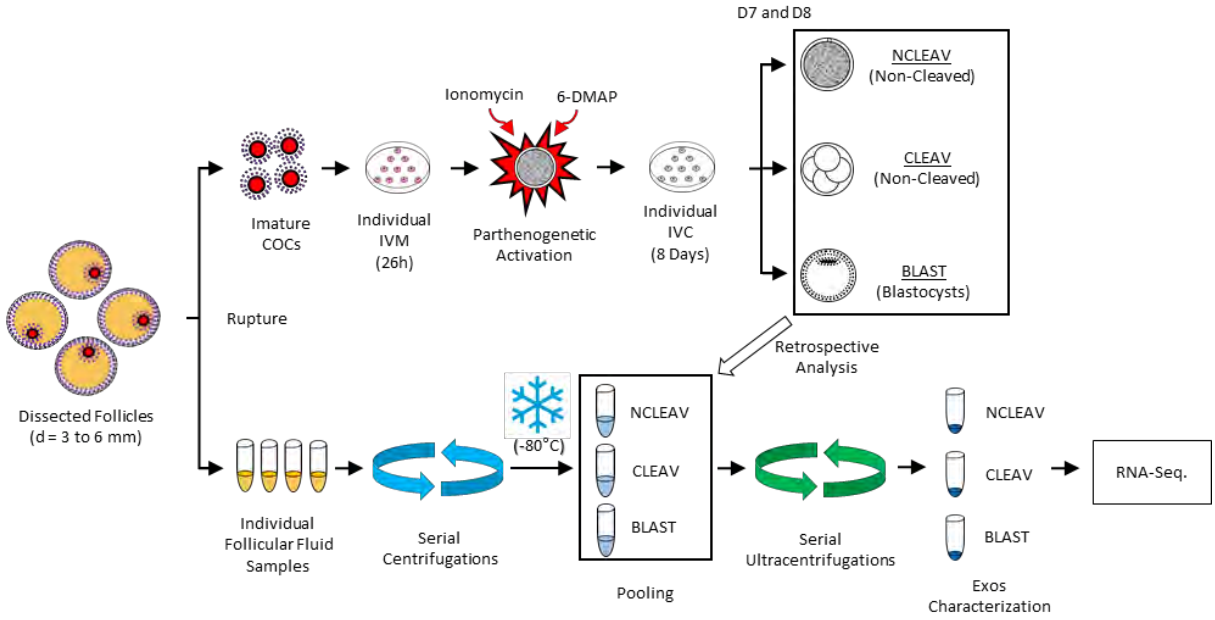

Figure 1. Experimental design.

2.1.3. Isolation of exosomes from the follicular fluid pools

The methods used for the isolation and characterization of the Exos, were previously described elsewhere (DA SILVEIRA et al., 2021). After the identification and separation of the COC, the follicular fluid of the individually isolated follicles were transferred to Eppendorf tubes (0.6 ml) and subjected to consecutive centrifugation steps. Briefly, follicular fluid samples were centrifuged at 300x*g* for 10min to remove live cells, at 2000x*g* for 10min to remove residual cells and cell debris, at 16500x*g* for 30min to pellet the EVs. The remaining supernatant was filtered through 0.2 mm sterile filter to remove particles whose size is more than 200 nm and centrifuged at 119700x*g* for 70 min. Following centrifugation supernatant

was changed by PBS (pH 7.4) to wash the pellet and centrifuged one more time at 119700x*g* for 70 min to pellet the exosomes (Exos). Centrifugation steps were performed at 4 ºC. Pellets were ressuspended in 50 mL of PBS. The Exos validation was acquired using Nanosight equipment (Malvern) and analyzed by NanoSight NTA Software v3.1. In order to determine the Exos size and distribution, 3 pellets were used. First 50 nm, 100 nm and 150 nm calibration beads (Malvern) were used to check size accuracy. EVs were diluted in PBS, introduced manually and analyzed by recording five videos of 30s. Videos were acquired at camera level 14 at 37 ºC. Vesicles size was defined as the mode determined from the acquired videos and vesicles concentration was defined as the mean determined from the videos. The data related to the EVs characterization can be found in Da Silveira et al. (2021).

2.1.4. RNA Extraction

The total RNA of the samples was extracted using the Trizol® reagent (Molecular Research Center, Cincinnati, OH) following the manufacturer's recommendations with slight modifications, such as the use of a small volume of Trizol (200 μL) and chloroform (128 μL), followed by purification of the aqueous phase in miRNeasy (Qiagen, #217084, Venlo, Limburg, Netherlands). RNA was dissolved in 10 μL of RNase free water and treated with DNaseI (Invitrogen, Carlsbad, CA). RNA concentration was measured with A260 measurements using NanoDrop 2000 (Thermo Scientific, Carlsbad, CA).

2.1.5. RNA sequencing

Additional EVs analyses and validation steps including transmitted electron microscopy, protein markers, lipid extraction and RNA isolation were performed previously thought using protocols described elsewhere (DA SILVEIRA et al., 2017, 2021). Briefly, after evaluating quality and quantity of RNA, the cDNA was synthesized using the commercial SMART-Seq® HT Kit (Takara Bio USA), and libraries were produced using the commercial Illumina Truseq Stranded mRNA Sample Prep Kit, as per the manufacturer's recommendations and validated by De Ávila et al. (2019). The total cDNA was quantified again using the Agilent Bioanalyzer 2100 (Agilent, Santa Clara, CA, USA), and quantified using quantitative PCR with the KAPA Library Quantification kit (KAPA Biosystems, Foster City,CA, USA). Only samples containing amplicons with size between 250 and 500 bp were considered acceptable. For each sample, between 10pg and 1ng of RNA samples were used for cDNA production and 200ng were used for library preparation. The libraries were sequenced on an Illumina platform and the data were analyzed according to a pipeline pre-established in our laboratory (DA SILVEIRA et al., 2017). Briefly, sequencing quality was analyzed with Fastqc, then filtered with TrimGalore, removing quality reads lower than 30 phred score. The result obtained was aligned with the reference genome using the latest version available in the ENSEMBL repository of *Bos taurus* (ARS-UCD1.2) and the count of reads belonging to each gene was obtained by the FeatureCounts method with the aid of the Rsubread R package, as recommended by the authors of the package (LIAO; SMYTH; SHI, 2019).

2.1.6. Modulation in Wnt signaling pathway/ β-catenin

After washing the ovaries in warm saline solution, the ovarian follicles between 3-6 mm were punctured with an 18 G needle and 10 mL syringe. Decanting the FF, COCs with homogeneous ooplasma and compact cumulus, were washed in TCM 199 medium (GIBCO) with HEPES buffer (20 mM), sodium bicarbonate (5 mM) and addition of sodium pyruvate. sodium (0.2 mM) and gentamicin (50 µg/mL). Also, 20 immature COCs were fixed with 4% paraformaldehyde for 15 min and stored for the following experiment. Then, COCs were washed in TCM 199 maturation medium (GIBCO) with 25mM sodium bicarbonate, supplemented with 10% FBS (Cripion Biotecnologia, Andradina, SP, Brazil) , sodium pyruvate (0.2 mM), gentamicin (50 µg/mL), follicle-stimulating hormone (FSH; 1 µg/mL; Folltropin-V; Bioniche Animal Health Belleville, Canada) and human chorionic gonadotropin (hcG ; 50 µg/ mL; Vetecor, Hertape Calier).

Groups of 20 to 25 COCs were distributed per well in the same maturation medium in 4-well plates (NUNC®) matured for 26 h of *in vitro* maturation (IVM), first 8 hours in maturation medium depleted of FSH/LH , in four conditions initially: Control DMSO 0.2%, CTL, chemical probe CHIR99021 (3 µM, Axon Medchem® 1386, dissolved in DMSO 99.7%,), CHIR, and DKK-1 protein (200 ng/mL, PeproTech® 120–30, according to manufacturer's recommendations), DKK1 and the fourth condition exposed the COCs to CHIR99021 for the first 8 h and then to DDK1 for the remaining 26h IVM period, C+D. The concentrations used here were based on works of Aparicio (2010) and Spate et. al (2014).

After the 19h of IVM, the COCs from the four conditions were denuded by fine-pipetting and returned to maturation medium with their respective treatments and were incubated until the activation protocol. Oocytes were classified into matured (IVM +) or non-matured (IVM -) based on the presence or absence of the first polar body (1st PB), respectively.

After 26 h of maturation, all oocytes were parthenogenetically activated, regardless of presence or not of a 1st PB. Oocytes were washed three times with H199 medium (TCM-199 with 25 mM HEPES) containing 0.5 mg/mL bovine serum albumin (BSA), 0.2 mM pyruvate, and 50 μg/mL gentamicin. After washing, oocytes were activated, using the same medium supplemented with 5mM ionomycin for 5 min.

Then, the oocytes were washed thrice with H199 saturated media (TCM-199 with 25mM Hepes containing 30 mg/mL BSA, 0.2 mM pyruvate, and 10 μg/mL gentamicin) and washed thrice right away with synthetic oviduct fluid (SOF) supplemented with 5 mg/mL BSA, 2.5% extracellular vesicles depleted-fetal calf serum (EVsfree-FCS), 0.2 mM pyruvate, 10 mg/mL gentamicin, and 2mM 6-dimethylaminopurine (6-DMAP). Finally, the oocytes were transferred into 90 μL drops of DMAP-supplemented SOF in 35mm plate covered with mineral oil and incubated at 38.5 ºC in a humid atmosphere of 5% O_2, 5% CO_2 and 90% N_2 for 3 h.

Following DMAP activation, oocytes were washed three times with SOF medium supplemented with 5 mg/mL BSA, 2.5% EVsfree-FCS, 0.2 mM pyruvate, and 10 μg/mL gentamicin, and subsequently cultured in 500 μL droplets of fresh culture medium covered with mineral oil in a new 4-well plate (NUNC®) at 38.5 ºC in a humid atmosphere of 5% O_2, 5% CO_2 and 90% N_2 for 8 days. The presumptive embryos were evaluated for cleavage at D3 (48 h) and for blastocyst development at D7 (168 h) post-activation.

2.1.7. β-catenin immunofluorescence analysis

To evaluate the treatments effects over the WNT signaling pathway of COCs and their respective cumulus cells (mCC) one biological replicate of the three conditions (CTL, DKK1 and CHIR), as described in the previous section, were perfomed and monitored by a β-catenin immunostaining analysis following Sampaio and collaborators immunostaining protocol (2015) with few modifications. Briefly, after the 19h of IVM-treatment, 20 to 25 COCs from the three conditions were partially denuded by fine-pipetting. Then, the COCs and their respective mCC were immediately fixed with 4% paraformaldehyde for 15 min and stored at 4 °C, the mCCs were plated on coverslips before fixation. In sequence, the cells (COCs and mCC) were permeabilized with D-PBS + 1% Triton X-100 for 10 min and blocked for 30 min in D-PBS + 0.3% Triton X-100 + 1% BSA, were placed in primary antibody solution consisting of blocking buffer, a mouse antibody anti- β-catenin —Abcam (ab1220, 1:500), overnight at 4 °C. Cells incubated without primary antibodies were used as negative controls for all assays. In the next day, after washing 3 × for 10 min each, cells were incubated with secondary antibodies Alexa Fluor 568-conjugated goat anti-rabbit IgG (Life Tech, cat. # A-11036 and Alexa Fluor 488-conjugate goat anti-mouse IgG (Life Tech, cat. #: A-11029) both at RT for 1 h. Then, after washing for 3 × for 10 min each, samples were mounted on microscope slides and with Prolong Gold Antifade Mountant (Life Tech, cat. # P36935). Images were captured using a confocal microscope (TCS-SP5 AOBS; Leica, Soims, Germany) using laser excitation and emission filters specific for Alexa 488 and Alexa 568. Digital images of mCC in each condition (CTL, DKK1 and CHIR) were analyzed using ImageJ-Fiji image processing software (National Institutes of Health, Bethesda, MD, USA) by evaluating each nucleus fluorescent intensity, 25 cells per experimental group were measured in randomly selected microscopic

fields. The fluorescent integrated density (average mean gray value) of each channel were measured by manually outlining each mCC nucleus and adjusted against background.

2.1.8. Statistical analyses

The analyses were performed using the public domain R software and its packages, which were necessary for data generation, graph construction and functional analysis of the transcripts. The gene expression difference analysis was performed following the recommendations and methodology contained in the DESEQ2 package (LOVE; HUBER; ANDERS, 2014) and the analysis of gene ontology (GO) and pathway enrichment for Encyclopedia of' Kyoto' Genes and Genomes (KEGG) was used the ClusterProfiler package both from the R software (KANEHISA; GOTO, 2000; YU et al., 2012).

For the developmental rates statistical analysis, Chi-square test was perfomed from R stats package graphics (R CORE TEAM, 2023). Immunostaining analysis was performed a linear mixed-effects model via maximum likelihood, lme4 (BATES et al., 2015), with Least Square of Means (emmeans) post-hoc test using the mixed model (LENTH, 2023).

2.2. RESULTS

From the retrospective experiment, were collected and individually activated one hundred seventy-four oocytes. To ascertain a homogeneity among samples, only routines with blastocyst rates greater than 35% had their follicular fluids used for exosomes (Exos) isolation and analysis (Table 1).

Table 1. Development rates of individual parthenogenetic bovine embryos displaying blastocyst/cleaved rates greater than 35%.

Routine	**Oocytes**	**Cleaved**	**Cleaved** (%)	**Blastocysts**	**Blastocysts** (% oocytes)	**Blastocysts** (% cleaved)
1	16	10	62.50	6	37.50	60.00
2	16	9	56.25	5	31.25	55.56
4	19	11	57.89	5	26.32	45.45
6	21	15	71.43	7	33.33	46.67
7	18	11	61.11	4	22.22	36.36
8	22	16	72.73	8	36.36	50.00
9	23	17	73.91	7	30.43	41.18
10	17	11	64.71	5	29.41	45.45
11	22	11	50.00	4	18.18	36.36
TOTAL	174	111	63.79	51	29.31	45.95

(ANDRADE et al., 2017)**.**

RNAseq was performed from three samples of Exos collected from bFF of follicles harboring competent (BLAST) and incompetent (CLEAV and NCLEAV) gametes. After trimming and filtering, the RNAseq generated a total of approximately 32,400,000 single reads (Figure 2A). With 85% alignment of these reads with the ENSEMBL genome of *Bos taurus* (ARS-UCD1.2), and a total of 36,488 genes detected. Classifying the transcripts by gene biotype indicated that most of the genes detected were protein coding (mRNAs), including transcription factors, and long non-coding RNAs (lncRNAs; Figure 2B), as expected. The other RNA biotypes had relatively lower counts. The mRNAs and lncRNAs proportions varied according to the gamete competence, NCLEAV group showed 6% more mRNAs (Figure 2C) and less lncRNAs (Figure 2D) in comparison with the BLAST and CLEAV groups. However, transcription factor mRNA counts showed no such differences (Figure 2E).

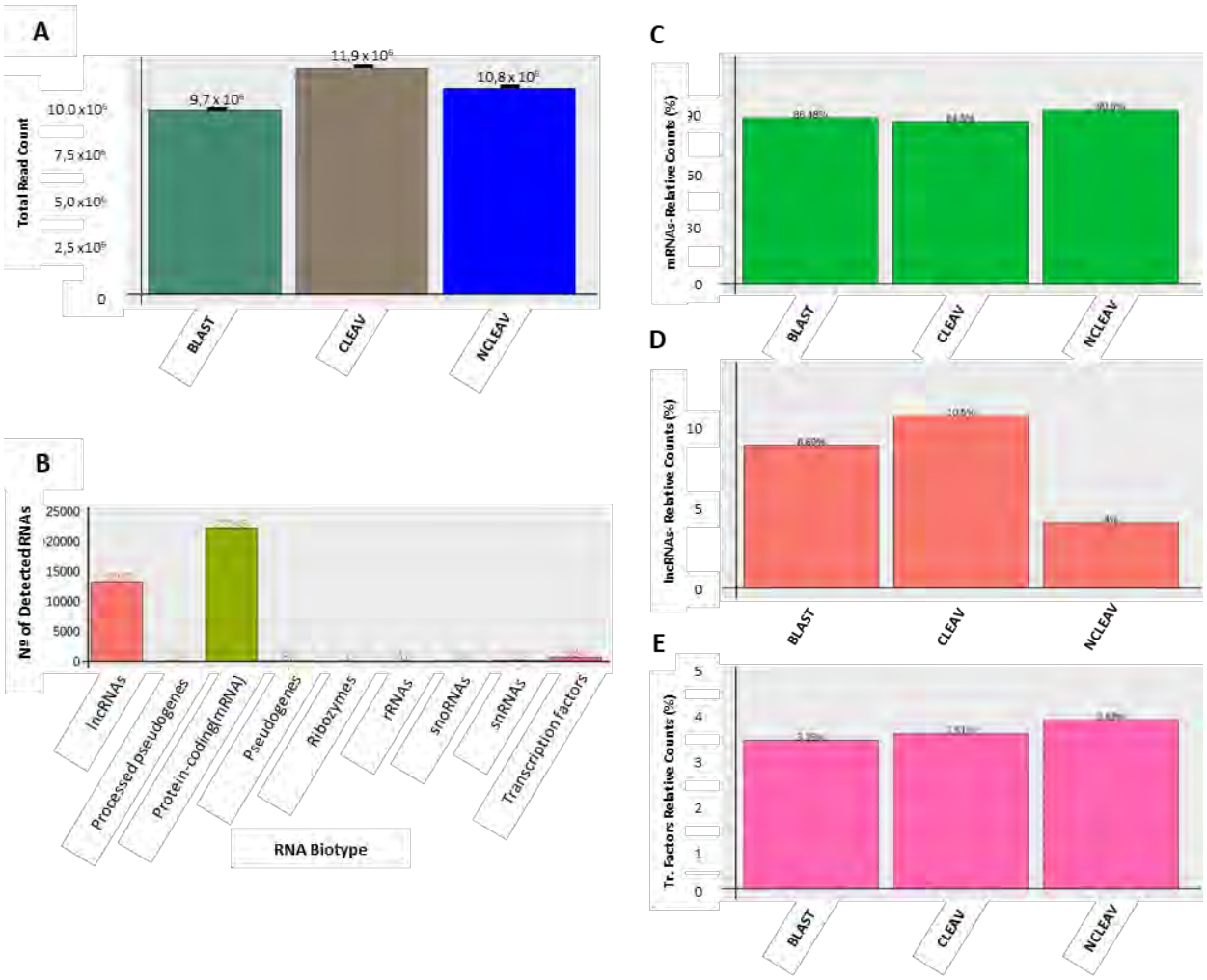

Figure 2. Overview of exosome reads showing (A) Total reads counts by experimental group, total reads values indicated at the top of the columns for the BLAST (Blastocysts), CLEAV (Cleaved) and NCLEAV (Non-cleaved) groups. (B) Number of gene transcripts per gene biotype. Relative percentages of the main gene biotypes (C) Protein coding (mRNAs), (D) lncRNAs and (E) Transcription factors among the groups.

2.2.1. Identification of differentially expressed genes in the exosomes

Differential gene expression analysis of the exosome-like vesicles pools identified 1,735 differentially expressed genes (DEGs, with |Log2(Fold Change)| > 1 and p-adj < 0.1). As illustrated on the smear plot (Figure 3A), transcript profiles from BLAST and CLEAV groups resulted in fewer DEGs identified in comparisons to the other groups. The comparison BLAST *vs.* NCLEAV (Figure 3B) revealed a higher volume of DEGs. A third comparison involving the NCLEAV and the CLEAV groups (Figure 3C), resulted in more DEGs than in BLAST *vs.* CLEAV comparison.

Principal Component Analysis of the DEGs (PCA; Figure 3D), corresponded to 72% of the variation. It was observed the presence of 2 main clusters of pools, the first cluster corresponds to the pools belonging to groups BLAST and CLEAV that were closest in terms of variance, while the second cluster consisted only of pools from the NCLEAV group, again differing from the others groups.

When organized in a Venn diagram (Figure 3E) the discrepancy becomes more tangible. Whereas the 229 DEGs, 13.2% from total, were detected in both the BLAST and the CLEAV groups, the NCLEAV shared only 111 DEGs (6.3%) with the other two groups. Overall NCLEAV group more similarity with the cleaved group, 73 DEGs (4.2%), compared to the BLAST group, 38 DEGs (2.2%).

The heatmap of relative gene expression by pool (Figure 2F) of the DEGs detected in the transcriptomic profile, visually demonstrated specific similarities between the profiles of the BLAST and CLEAV groups. The NCLEAV group, in turn, demonstrated a high number of DEGs generally discordant from both CLEAV and BLAST.

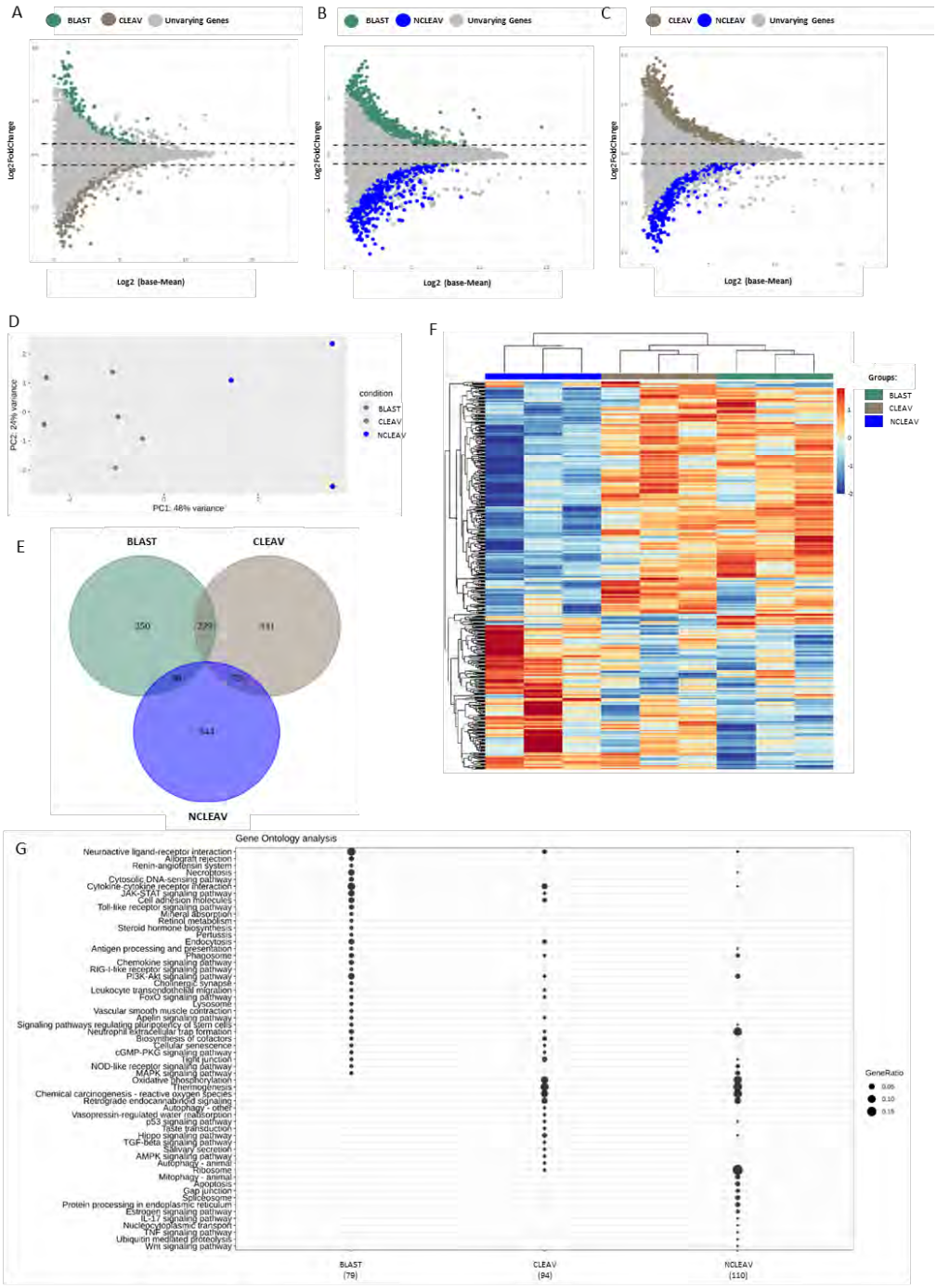

Figure 3. Differential gene expression analyzed using the "DESeq2" package of the R software. The smear plots represent the DEGs between the experimental groups: (A) BLAST vs. CLEAV, (B) BLAST vs. NCLEAV and (C) CLEAV vs. NCLEAV. With |Log2(Fold Change)| > 1 the gray dots indicate genes that did not vary in their expression between the groups (p-adj <0.1), the green dots indicate the most expressed DEGs in the BLAST group and the brown dots the CLEAV group DEGs and the blue ones the NCLEAV group with p-adj < 0.1. (D) Principal Component Analysis (PCA) Plot considering only the DEGs between groups BLAST, CLEAV and NCLEAV. (E) Venn Diagram with the DEGs counts by experimental group, the overlaps indicate the DEGs detected at similar transcriptional levels between overlapping groups but which differed from the non-overlapping group. (F) Heatmap hierarchically grouping DEGs between pools, NCLEAV vs. CLEAV vs. BLAST groups, identified respectively by the blue, brown and green bands at the top of the heatmap. The color scale bar shows changes in relative gene expression normalized by standard deviation (0 is the mean expression of a given gene in this study). (G) Gene Ontology (GO) analysis for KEGG, the size of each bubble shows the ratio between the number of DEGs found in the present study belonging to the functional categories and the total number of genes in the functional categories per experimental group, shown at the bottom of the chart.

Performing a cluster analysis for Kyoto Encyclopedia of Genes and Genomes (KEGG) database, the gene ontology (GO) identified DEGs associated with several biomolecular functions (Figure 3G). The analysis detected 283 DEGs, with 110 genes present in follicular exosomes (Exos) from NCLEAV group were the group which presented more DEGs, followed by CLEAV exos with 94 genes and BLAST Exos with 79 genes.

Few functions were found only in the BLAST group, mostly with a low gene ratio, thus possibly associated with the capacity to reach blastocyst stage. The most relevant functions ranging from 15% to 10% of the DEGs included neuroactive ligand-receptor and cytokine-cytokine receptor interactions. From 10% to 5% of gene ratio, PI3K-Akt, JAK-STAT signaling pathways, necroptosis and endocytosis were the most relevant molecular functions (MFs) detected. With 5% or less genes, some relevant MFs presented DEGs only in the BLAST group, such as steroid hormone metabolism, renin-angiotensin system and vascular smooth muscle contraction. However, in general, the MFs were associated with decreased DEGs on CLEAV and/or NCLEAV groups.

The functional categories associated with the inability to reach the blastocyst stage in both CLEAV and NCLEAV group, using the criteria of 15 to 10% of the gene ratio, were thermogenesis, oxidative phosphorylation (OXPHOS) and chemical carcinogenesis associated with reactive oxygen species (ROS). Presenting 5% or less of the gene ratio, some DEGs corresponded to p53 and hippo signaling pathways.

Finally, in the NCLEAV group, ribosomal functions and formation of extracellular neutrophil traps were more associated with the inability to cleave, presenting 15% and 10% of the group's gene ratio. Some relevant MFs were restricted to the incompetence such as apoptosis, gap junctions and estrogen signaling pathway, all representing 5% or less of the DEGs detected in the NCLEAV. Interestingly, also with 5% of the DEGs ratio, MAPK and

NOD-like receptor signaling pathways shared only between NCLEAV and BLAST groups, other MFs with the same characteristic represented less than 5%.

2.2.2. Detected HUB genes description

After identifying the DEGs, we focused our analyses over the pathways and specific genes that may be related to oocyte competence, clustering 36 HUB genes with Transcripts per million (TPM) log2 fold change ≥ -0.5 and p-adj <0.1, emphasizing signaling pathways previously associated to gamete competence, such as PI3K-Akt, Hippo and Wnt signaling pathways (GROSBOIS; DEMEESTERE, 2018; MARTÍNEZ-MORO et al., 2022) and other twelve modules considered peripheral for this study (Figures 4A).

The majority of genes were overexpressed in BLAST and CLEAV groups. More specifically, 18 genes (*FZD1, COL1A1, DVL1, BMP8A, WNT9B, ERBB3, SCRIB, LAMB2, AKT1, SMAD7, GLI2, WTIP, RXRA, PIK3CD, AXIN2, CSF1, NOS3* and *PARD6G*) were more expressed in the BLAST group and 16 genes (*LPAR6, FGF18, ID1, FGF18, BMP8B, CCND1, COL2A1, STK11, DVL2, ITGA7, TP73, ITGA5, TEAD4, FGFR4, APC2A and LLGL1*) were more expressed the CLEAV group. Notably, for this analysis, *MCL1* (Myeloid Cell Leukemia-1) was clearly the only gene found to be more expressed in the NCLEAV group than the other two experimental groups. The *IBSP* (Integrin-Binding Sialoprotein) gene was also overexpressed, but in both NCLEAV and BLAST groups, whereas other genes in NCLEAV group were predominantly sub-expressed or maintained their mean expression.

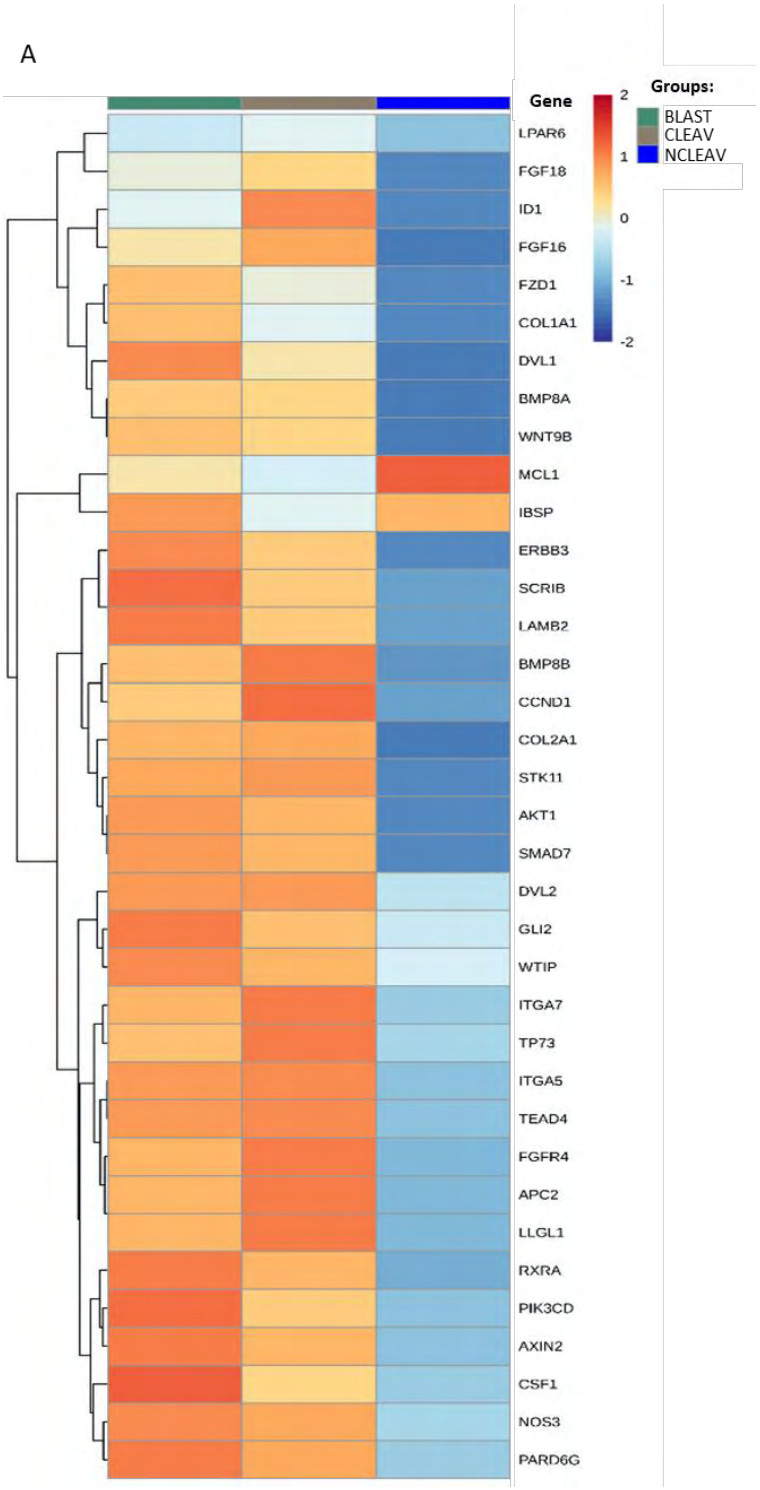
A
Gene
Groups:
BLAST
CLEAV
NCLEAV
2
1
0
-1
-2
LPAR6
FGF18
ID1
FGF16
FZD1
COL1A1
DVL1
BMP8A
WNT9B
MCL1
IBSP
ERBB3
SCRIB
LAMB2
BMP8B
CCND1
COL2A1
STK11
AKT1
SMAD7
DVL2
GLI2
WTIP
ITGA7
TP73
ITGA5
TEAD4
FGFR4
APC2
LLGL1
RXRA
PIK3CD
AXIN2
CSF1
NOS3
PARD6G

B

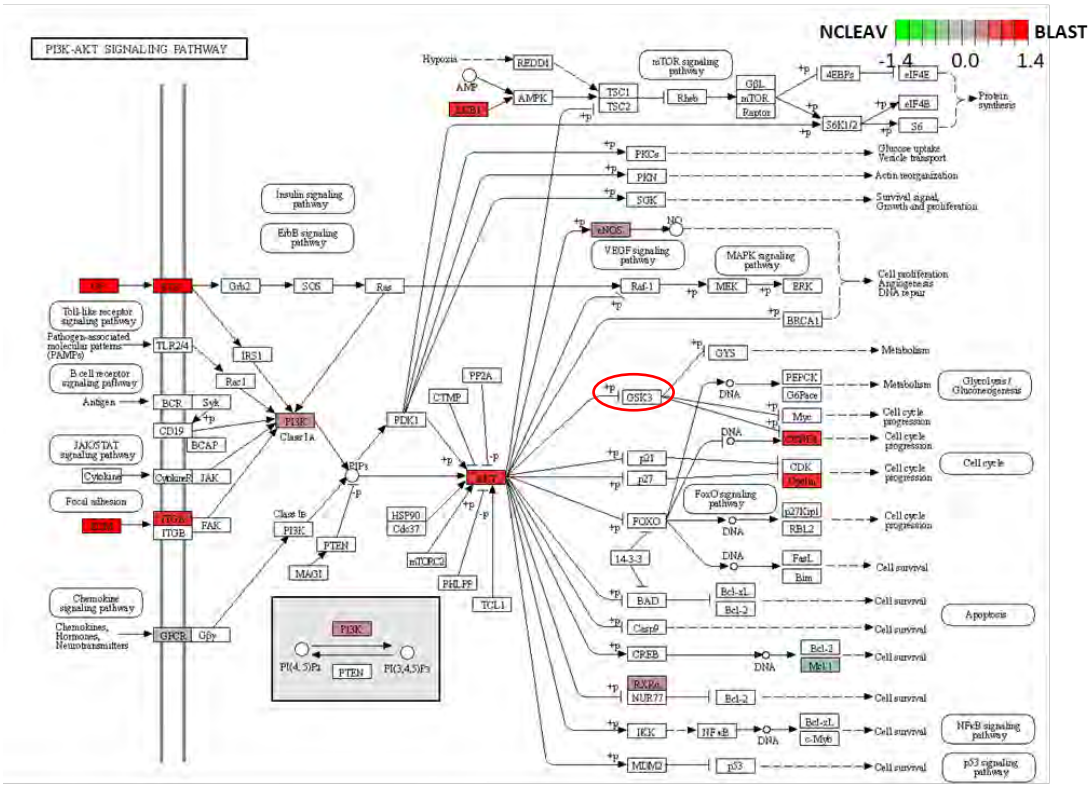

C

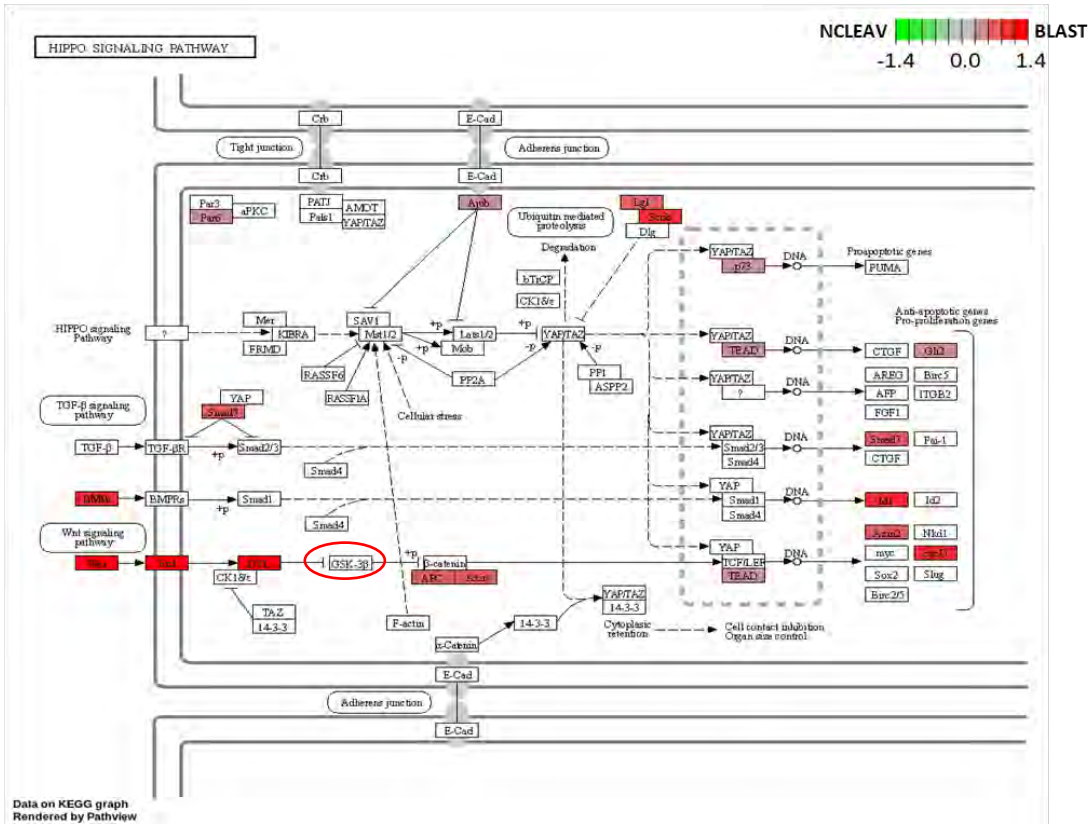

Figure 4. Analysis between signaling pathways related to oocyte competence and HUB genes transcripts detected in the exosomes of experimental groups. Heatmap hierarchically grouping HUB genes related to PI3K-Akt/Hippo/WNT pathways in the BLAST, CLEAV and NCLEAV groups (C). Pathview visualization for PI3K-Akt signaling (B) and Hippo (C) signaling pathways enriched in the exos transcripts (HUB genes) from a BLAST/NCLEAV comparison. Contrasts the BLAST (red) vs NCLEAV (green). (q<0.1).

Aiming to enhance the contrast of the different profiles, the exos transcriptomic content from BLAST and NCLEAV groups were compared and contrasted through these HUB genes for (Figure 4B) and Hippo (Figure 4C) signaling pathways. Hence, with this comparison between the most competent group and the less competent group revealed important genes well distributed along the PI3K-Akt signaling pathway, such as *PIK3CD, AKT1* and *CCND1*. Interestingly, in the Hippo pathway analysis it is clearly notable a highlighting of genes associated with Wnt signaling pathway, such as *WNT9B, FZD1, DVL1/2, AXIN2, APC2 and TEAD, in* more than a few levels of the pathway. Several of these genes were proportionally related to the capacity of the oocyte to reach blastocyst stage, thus, more expressed in the BLAST group. In addition, it came to our attention a GSK3β *(Glycogen Synthase Kinase 3 β)* possible activity in the follicular niche appeared to be a key factor between the PI3K-Akt, Hippo and Wnt pathways (DUDA et al., 2020; HENG et al., 2020). Suggesting a transcriptional stimulation of these signaling pathways in the follicular environment made by the exos.

2.2.3. Development rates after GSK3β modulators treatments

Based on the above results and to investigate GKS3β key function in PI3K-Akt and Wnt signaling pathways, we matured COCs for 26 hours under the 4 conditions: CTL, Control group with DMSO; DKK1, treatment that indirectly stimulates GSK3β by inhibition of the WNT signaling pathway through DKK-1 (Dickkopf related protein 1) that blocks Wnt ligands to interact with membrane receptors (KAGEY; HE, 2017); CHIR, treatment that directly inhibits GSK3β through the chemical probe CHIR9902 (APARICIO et al., 2010); C+D, treatment using CHIR99021 for the first 8 hours to impair the 1st polar body extrusion and other 18 hours with DKK1. The first 8 hours in maturation medium depleted of FSH/LH and, in the fourth group, with CHIR99021 were used in attempt to reduce external interference over the oocytes maturation.

Table 2. Development rates of bovine oocytes/embryos, obtained from treatments with GSK3β modulators.

Group	**n**	**1st PB Extrusion** (%±Standard Error)	**Cleavage** (%±Standard Error)	**Blastocyst** (%±Standard Error)	**Nº Blastocysts Counted**	**N° of Cell / Blasctocyst** (±Standard Error)
CTL	9	70.7 ± 3.2	84.4 ± 2.7	45.1 ± 2.1	37	159.3 ± 10.5
DKK1	9	64.5 ± 2.6	79.5 ± 3.6	45.7 ± 4.0	27	144.9 ± 12.1
CHIR	9	83.3 ± 1.8*	82.8 ± 2.7	36.0 ± 2.5	36	139.8 ± 10.3
C+D	9	69.1 ± 2.2	82.1 ± 2.8	38.5 ± 3.1	20	160.7 ± 8.3

1st PB: First polar body.

*P<0.05

A

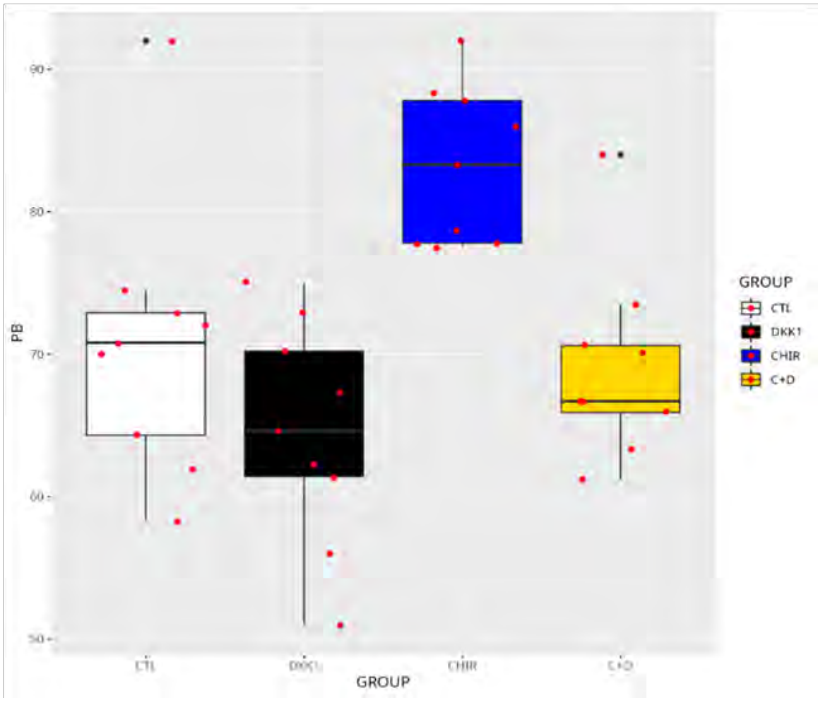
PB
90
80
70
60
50
CTL
DKK1
CHIR
C+D
GROUP
GROUP
CTL
DKK1
CHIR
C+D

B

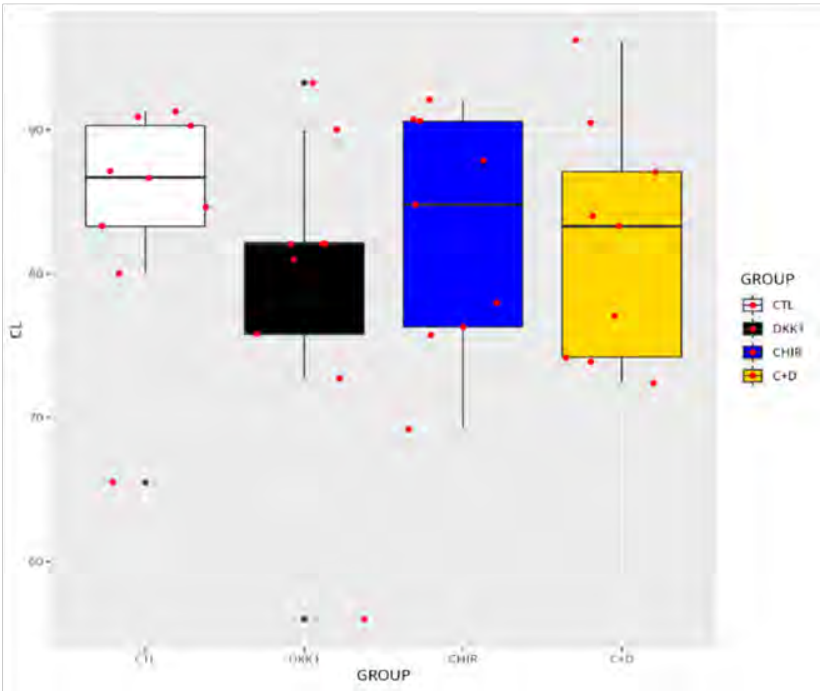
CL
90
80
70
60
CTL
DKK1
CHIR
C+D
GROUP
GROUP
CTL
DKK1
CHIR
C+D

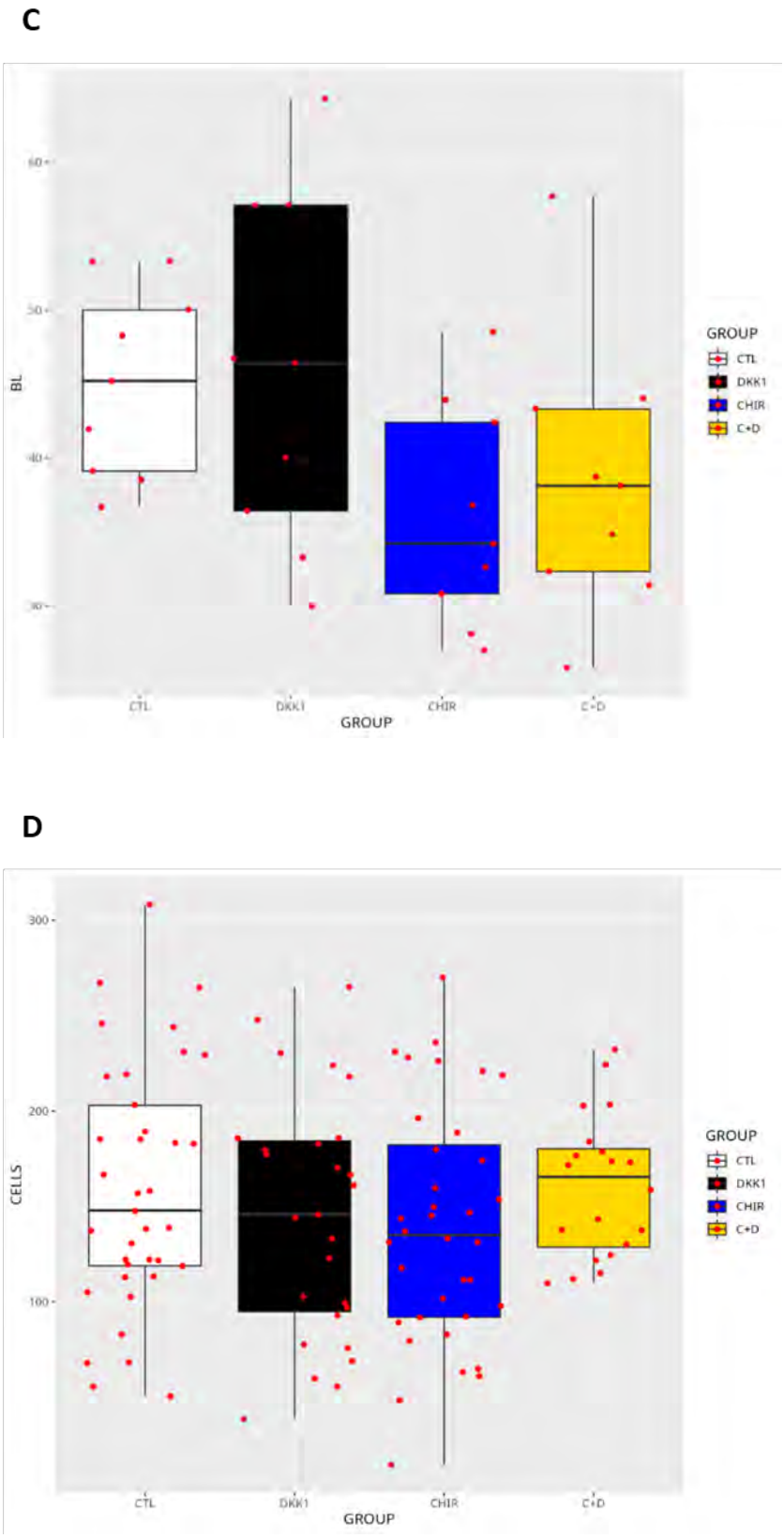

Figure 5. Boxplots graphs of the developmental rates obtained from GSK3β modulators treatment. (A) 1st PB extrusion rates (PB), (B) cleavage rates (CL), (C) Blastocyts (BL) rates and (D) cell number per blastocyst (CELLS). The red dots represent the repetitions or cell counts in each blastocyst. Treatment groups are represented by white (CTL), black (DKK1), blue (CHIR) and yellow (C+D) boxes, ($p<0.05$).

Developmental rates of 1758 COCs, 50 to 60 COCs per treatment. were used to investigate the treatments effect on development (Table 2). Interestingly, CHIR group, showed higher 1st PB extrusion rates ($p<0.05$) compared to the other three groups (Figure 5A). However, no differences were observed on cleavage (Figure 5B), blastocyst (Figures 5C) rates and blastocyst cell number (Figures 5D).

2.2.4. Cumulus-oocyte complex suscept GSK3β modulators treatments

In view of our developmental results, we considered a validation of effectiveness of the CHIR99021 in the COCs. Thus, a experiment using immunostaining for β-catenin, a canonical member of the Wnt signaling pathway and related to the GSK3β activity (AKINO et al., 2020; ASUNI et al., 2006), were performed in matured COC under 3 previously described conditions (CTL, CHIR and DKK1) and also in intact immature COCs immediately fixed after aspiration.

The collected matured COCs and their respective cumulus cells (mCC) were immunostained for β-catenin, and the nuclei with HOECHST33342, a negative control was also established (Figure 6A). From these cells, the immature group showed β-catenin localized predominately in the mCC and oocyte cytoplasms (Figure 6B). Additionally, a similar visual pattern was observed in matured COCs from CTL group (Figure 6C), including oocytes nuclei. Although the DKK1 oocytes nuclei had presented similarities with CTL oocytes (Figure 6D), both mCC and oocytes treated with DKK-1 demonstrated a certain interference on β-catenin presence. Additionally, the CHIR group visually presented a higher intensity of β-catenin fluorescence in the mCC nuclei than the CTL group, the same effect occurred for COCs treated with CHIR99021 (Figure 6E).

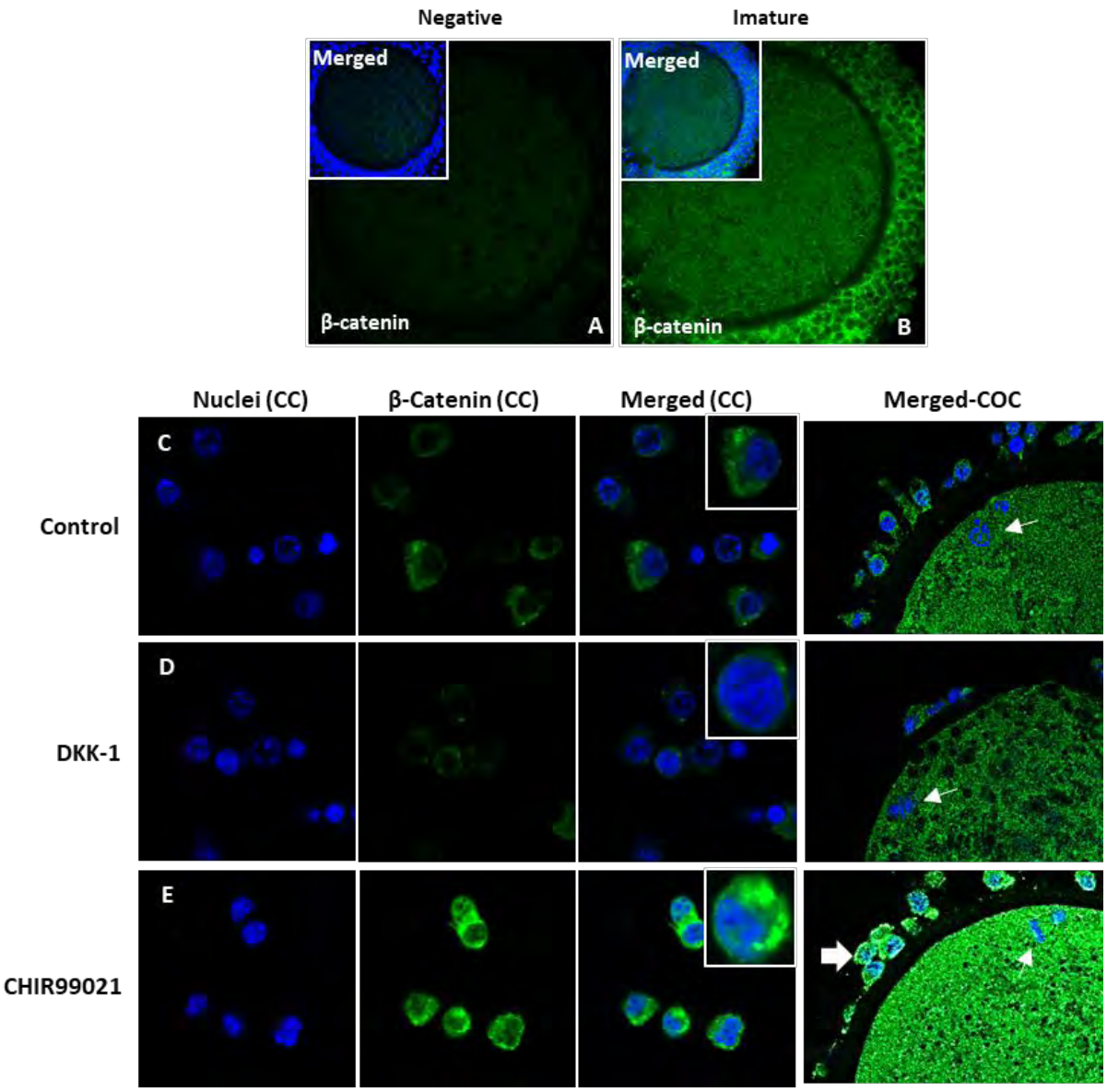

Figure 6. Representative pictures of Immunostaining for β-catenin (green), cell nuclei HOECHST33342 staining (blue) in cumulus cells (CC) and cumulus-oocytes complexes (COCs). (A) Negative-Control for β-catenin and (B) intact and immature COCs with their merged visualization. Pictures after 26h in maturation medium on three conditions: (C) CTL (Control), (D) DKK1 (DKK-1) and (E) CHIR (CHIR99021) treatments. The small white arrow on the digital zoomed COCs after treatment points their nuclei and the large white arrow on the CHIR COC indicates its respective CC nuclei. Photographs were acquired 63 x objective.

To analyze the differences observed between from CTL group and treated groups, we measured the integrated densities of the nuclei and nuclear β-catenin fluorescence from these mCC groups. From these analyzes, we detected an increase of the HOECHST33342 integrated density (IntDens) in the cells from the DKK1 group, keeping the majority of values around $8.9x10^6$ pixels ($p\text{-value} < 0.05$), while the CTL and CHIR kept values concentrated around

$5x10^6$ pixels (Figure 7A). Moreover, the measurement of the nuclear area delimited by HOECHST33342 revealed an increase of the mCC nuclear area in response to DDK1 treatment in contrast with CHIR treatment (p-value < 0.05) but both groups did not presented statistical difference when compared to the CTL group (Figure 7B).

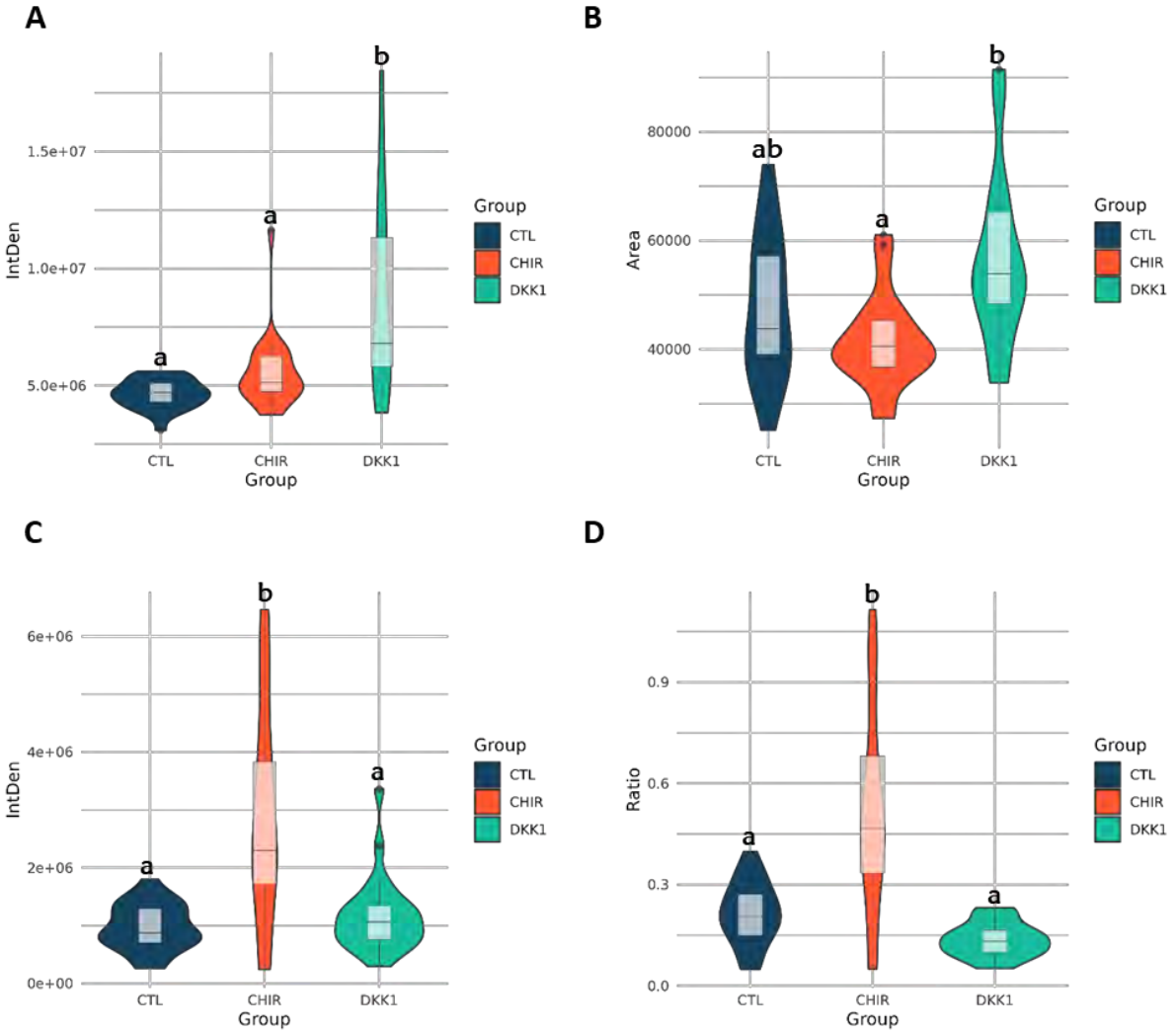

Figure 7. Immunostaining nuclear integrated density analysis after GSK3β modulators treatment. Violin Charts comparisons of cumulus cells collected from oocytes after 26h in maturation medium (mCC) on three conditions: Control CTL (blue), CHIR99021 and DKK-1 CHIR (orange) and DKK-1 (green) experimental groups shown at the x axis. The y axis shows four analysis: (A) Integrated Density (IntDens) in pixels for HOECHST33342 staining, (B) Nuclear Area (HOECHST33342), (C) IntDens in pixels for β-catenin immunostaining and (D) Nuclear integrated density ratios (β-catenin /HOECHST33342) for each group. The colored structures around the boxplots represents the distribution of repetitions, mCCs, measured in each group (p-value < 0.05). Integrated densities were calculated by multiplying the nuclear area by the mean gray value of the pixels within.

Intriguingly, CHIR99021 group presented a notable increase of nuclear β-catenin IntDens with values above $2x10^6$ pixels (p-value < 0.05), while the CTL and DKK1 cells showed values around $1x10^6$, with no statistical difference between them (Figure 7C). Furthermore, when nuclear integrated densities ratio were calculated between β-catenin and HOECHST33342 fluorescence (β-catenin / HOECHST33342) the mCC from CHIR99021 group presented the highest ratio values, ≈ 0.45 (p-value < 0.05), than the cells from CTL and DKK-1 treated groups, but not between them (Figure 7D). Noteworthy, both DKK1 and CHIR cells, when with statistically different values from the other groups in the respective analyses, presented a less accentuated clustering and a wider distribution of values.

2.3. DISCUSSION

Extracellular vesicles (EVs) are secreted by the majority of eukaryotic cells and significantly participate in several pathological and physiological processes (KOWALCZYK et al., 2022). In this study, we analyzed the poly A RNA content of exosomes (Exos) derived from ovarian follicular fluid pools classified through a bovine retrospective model developed in our laboratory. This model separates the samples into different competence levels based on *in vitro* embryonic development resulting from individually matured, parthenogenetically activated oocytes *in vitro*. Bioinformatics analysis revealed the abundant content of RNAs, especially lncRNAs and mRNAs, within these Exos, associated with numerous pathways associated directly or indirectly with the oocyte's capacity to develop to the blastocyst stage.

Likewise other Exos components (proteins, enzymes, lipids and nucleic acids), the profile of the exosomal RNAs depends on the physiological state and role of the original cell type (KOWALCZYK et al., 2022). Here we focused our attention on poly-A RNAs in bFF-derived Exos, such as mRNAs and lncRNAs. These RNAs biotypes presence in Exos, as other transcripts, are well documented (KIM et al., 2013; MATHIVANAN et al., 2012;

VEZIROGLU; MIAS, 2020; ZHANG et al., 2019). Also in cattle, previous studies revealed that milk-derived Exos containing mRNAs of key genes related to mastitis inflammatory response and lncRNAs that regulate pathways related to reproduction, cell proliferation and cell to cell communication, for example (JING et al., 2021; ZENG et al., 2019).

Abundant content of mRNAs stimulating pathways linked in different levels with oocyte quality and early embryo development were detected in Exos derived from both bovine and porcine follicular fluids (HASAN et al., 2020; MATSUNO et al., 2019). Recently, exosomal lncRNAs analysis derived from human follicular fluid detected differentially expressed genes (DEGs) between healthy women and women with polycystic ovary syndrome (PCOS), suggesting that lncRNAs could mediate the PCOS pathogenesis and used as biomarkers for the its diagnosis (WANG et al., 2021).

This work investigated the relation of the Exos Poly-A RNA content in the follicular fluid to the gamete competence, applying a model that unequivocally estimates the gamete potential to reach the blastocyst stage. The retrospective model, was previously used for studies of transcripts present in oocyte cytoplasmic biopsies and cumulus cells in relation to development competence (BIASE et al., 2012; MARTÍNEZ-MORO et al., 2022).

The use of small follicles derived exos has been shown to improve the *in vitro* development of embryos in cattle (DA SILVEIRA et al., 2017). However, it is important to note that in a pool of follicles there are Exos derived from follicular fluid of follicles containing high-quality oocytes capable of reaching the blastocyst stage as well as those derived from oocytes capable only of starting cleavage and finally to those not able to cleave. Therefore, it is important to understand the biology of these Exos before proposing their use to improve the production of embryos on a regular basis.

Herein, we identified a variety of molecular functions (MFs) associated with differentially expressed genes in the Exos retrospective groups. Around 15% of the genes were associated with neuroactive ligand-receptor interactions on the BLAST group and this percentage decreased jointly with the competence level on DEGs. Interestingly, most of these genes associated with neuroactive ligand-receptor interactions by KEGG annotation in our analysis also act in cell proliferation and differentiation. A good example is the *FDZ1*, Frizzled-1 protein, gene detected in the BLAST group as one of the most overexpressed HUB genes in the same group for PI3K-AKT and Wnt Pathways. This gene decodes a receptor for Wnt signaling pathway that regulates neurogenesis, the pathway also is related to oocyte maturation and embryo development (MARDONES et al., 2016; SAMEREH et al., 2021).

As for the CLEAV group, *ID1* was the most remarkable differential expressed gene in this group. *ID1* expression enhances cell resistance to DNA damage-induced apoptosis (ZHAO et al., 2016) and is related to the amount of SOX2 and other reprogramming related oocyte genes in low Ca++ nuclear transfer study (MENG et al., 2021).

The NCLEAV group had the most different profile of MFs of the DEGs in comparison with the other groups, genes that probably were aberrantly expressed genes. Similarly MFs were found altered in the transcriptomic content of human Exos with same origin (HU et al., 2020) and were detectable in GCs of Chinese buffalos (PAN et al., 2021). Thus, corroborating to the hypothesis of different transcriptomic profiles, especially between the BLAST and NCLEAV groups.

Therefore, the higher number of exclusive gene transcripts related to these cellular mechanisms in the Exos content of the BLAST group can indicate a cross talk between the COCs and the other follicular cells, suggesting that Wnt signaling and other communications pathways may be already active in the follicular environment and the COC as well. However, the results suggest that DEGs were aberrantly expressed in CLEAV and NCLEAV groups.

In regard to the findings and the influence of the interaction between and COCs in transcriptional level on the oocytes competence, the data obtained from DEG analysis in demostrated accordance with the literature (ANDRADE et al., 2017; MACHTINGER; BACCARELLI; WU, 2021; REGASSA et al., 2011)

Interestingly, the transcripts of the Phosphatidylinositol-4,5-bisphosphate 3-kinase catalytic subunit delta (PI3KCD) and AKT serine/threonine kinase 1 (AKT1) genes were also increased in the BLAST group ($q<0.1$). These two mRNAs by themselves encode a PI3K protein and a AKT protein, respectively. This result corroborates with previous works that detected these mRNAs in oocytes (CORNET-BARTOLOMÉ et al., 2021)and GCs (HUNG et al., 2017). Also support the facts that the PI3K-Akt signaling pathway transcripts are carried by the EVs and play an essential role in the oocytes competence acquisition and follicular development, not only in bovines but also in humans and pigs (ANDRADE et al., 2017; MACHTINGER; BACCARELLI; WU, 2021; MATSUNO et al., 2019; UZBEKOVA et al., 2020). These findings indicate that the model is coherent with the previous studies and corroborates to the validation of the experimental design. Moreover, it is in agreement to what is known to date about the origin and biological functions of Exos (BAZZAN et al., 2021; DA SILVEIRA et al., 2012; SOHEL et al., 2022).

The PI3k-Akt pathway is related to follicular quality and oocyte competence in many species such as cattle, swine and humans models, and its alteration is detrimental to oocyte quality (ANDRADE et al., 2017; DU; CHEN, 2021; JIAO et al., 2020). Since both pathways (PI3K and Wnt) relay on the GSK3 enzyme, a multifaceted kinase that plays a critical role in both the canonical pathways in order to control genes related to survival, neurogenesis and follicular development (SHORNING et al., 2020; VALVEZAN; KLEIN, 2012). We hypothesized that the GSK3β may play an important role on the maturation process and on developmental competence. To test the effect of this pathways and GSK3β on the oocyte

maturation we used two different strategies previously applied to oocyte maturation and embryo culture: direct GSK3β inhibition by CHIR99021 (BARROSO; CURCIO; DIAS, 2020) and an indirect stimulation by a WNT inhibitor DKK1 (SPATE et al., 2014).

Interestingly, although DKK1 treatment did not presented effect on development rates and B-catenin activity, the indirect stimulation by DKK1 promoted an increase of area and quantity of DNA. These results suggest a possible intensification of DNA synthesis in the DKK1 group in comparison with the two others groups, also indicative of the resumption of the cumulus-cells cycle. This phenomenon could be related to the activation of a non-Wnt signaling pathway by DKK1, where it binds to CKAP4 (cytoskeleton-associated protein 4) receptor and then activates PI3K-Akt signaling, simultaneously inhibiting GSK3β activity and stimulating cell proliferation (HERMIDA; DINESH KUMAR; LESLIE, 2017; KAGEY; HE, 2017).

Overall, the GSK3β inhibition by CHIR99021 resulted in an increase of the first polar-body extrusion with consequent increase in the maturation rate. These results are not in agreement with previously published articles that used Lithium (UZBEKOVA et al., 2009) and CHIR99021 (BARROSO; CURCIO; DIAS, 2020) that reported a decreased rate of maturation associated to the inhibition of the GSK3β. Both studies describe that, besides the effect on MII rate, such treatments did not result in greater blastocyst rate or better embryos based on the number of nuclei. In order to test if the inhibitor effect was effective we examined β-catenin localization as performed previously. Indeed, we were able to show that treatment with CHIR99021 increased the presence β-catenin in the nuclei of the cumulus cell that also showed a higher ratio of β-catenin /HOECHST33342 in the nuclei. Summarizing, the GSK3β inhibition suggests an increase in MII oocytes incompetent to develop to the blastocyst stage, that had an also increased β-catenin localization in the cumulus cells nuclei after maturation. Altogether, these characteristics exhibited by the CHIR group are similar to that previously shown in

human *in vivo* matured oocyte uncapable to develop to embryos and referred as dysmature oocytes, a term also used describe their respective follicles (AKINO et al., 2020; KANG et al., 2022; LOBO; DIZEREGA; MARRS, 1985).

2.4. CONCLUSION AND PERSPECTIVE

Taken together, our results unveiled many genes RNAs present in follicular fluid Exos that are related to the gamete's competence to develop up to blastocyst stage. In order to confirm the differences between the groups detected by transcript analysis we selected relevant proteins linked to the PI3K-Akt and Wnt signaling pathways previously identified in our group studies.

The modulation of GKS3β in COCs increased 1ºst PB extrusion rates. However the greater maturation rate didn't reflected on blastocysts rate. Since the treatment interfered in β -catenin localization in the cumulus cells. It is tempting to speculate that the treatment resulted increased dysmature gametes rates. Furthers studies are needed to confirm this speculation.

3. REFERENCES

AERTS, J. M. J.; BOLS, P. E. J. Ovarian follicular dynamics: A review with emphasis on the bovine species. Part I: Folliculogenesis and pre-antral follicle development. **Reproduction in Domestic Animals**, *[S. l.]*, v. 45, n. 1, p. 171–179, 2010. DOI: 10.1111/j.1439-0531.2008.01302.x.

AKINO, Ryosuke et al. Next-Generation Sequencing Reveals Downregulation of the Wnt Signaling Pathway in Human Dysmature Cumulus Cells as a Hallmark for Evaluating Oocyte Quality. **Reproductive Medicine**, *[S. l.]*, v. 1, n. 3, p. 205–215, 2020. DOI: 10.3390/reprodmed1030016.

ALBERTINI, David F.; COMBELLES, Catherine M. H.; BENECCHI, Elizabeth; CARABATSOS, Mary Jo. Cellular basis for paracrine regulation of ovarian follicle development. **Reproduction**, *[S. l.]*, v. 121, n. 5, p. 647–653, 2001. DOI: 10.1530/rep.0.1210647.

ANDRADE, Gabriella Mamede; DA SILVEIRA, Juliano Coelho; PERRINI, Claudia; DEL COLLADO, Maite; GEBREMEDHN, Samuel; TESFAYE, Dawit; MEIRELLES, Flávio Vieira; PERECIN, Felipe. The role of the PI3K-Akt signaling pathway in the developmental competence of bovine oocytes. **PLoS ONE**, *[S. l.]*, v. 12, n. 9, p. 1–15, 2017. DOI: 10.1371/journal.pone.0185045.

APARICIO, I. M.; GARCIA-HERREROS, M.; FAIR, T.; LONERGAN, P. Identification and regulation of glycogen synthase kinase-3 during bovine embryo development. **Reproduction**, *[S. l.]*, v. 140, n. 1, p. 83–92, 2010. DOI: 10.1530/REP-10-0040.

ASUNI, Ayodeji A.; HOOPER, Claudie; REYNOLDS, C. Hugh; LOVESTONE, Simon; ANDERTON, Brian H.; KILLICK, Richard. GSK3α exhibits β-catenin and tau directed kinase activities that are modulated by Wnt. **European Journal of Neuroscience**, *[S. l.]*, v. 24, n. 12, p. 3387–3392, 2006. DOI: https://doi.org/10.1111/j.1460-9568.2006.05243.x. Disponível em: https://onlinelibrary.wiley.com/doi/abs/10.1111/j.1460-9568.2006.05243.x.

BARROSO, Laura Mathias; CURCIO, Alinne Glória; DIAS, Angelo José Burla. Maturação in vitro de oócitos bovinos é negativamente afetada por CHIR99021, inibidor específico de GSK3. **Revista Brasileira de Reprodução Animal**, *[S. l.]*, v. 44, n. 4, p. 150–158, 2020. DOI: 10.21451/1809-3000.rbra2020.011.

BATES, Douglas; MÄCHLER, Martin; BOLKER, Ben; WALKER, Steve. Fitting Linear Mixed-Effects Models Using lme4. **Journal of Statistical Software**, *[S. l.]*, v. 67, n. 1, p. 1–48, 2015. DOI: 10.18637/jss.v067.i01. Disponível em: https://www.jstatsoft.org/index.php/jss/article/view/v067i01.

BAZZAN, Erica et al. Critical review of the evolution of extracellular vesicles' knowledge: From 1946 to today. **International Journal of Molecular Sciences**, *[S. l.]*, v. 22, n. 12, 2021. DOI: 10.3390/ijms22126417.

BIASE, Fernando Henrique; EVERTS, Robin Edward; OLIVEIRA, Rosane; SANTOS-BIASE, Weruska Karyna Freitas; FONSECA MERIGHE, Giovana Krempel; SMITH, Lawrence Charles; MARTELLI, Lúcia; LEWIN, Harris; MEIRELLES, Flávio Vieira. Messenger RNAs in metaphase II oocytes correlate with successful embryo development to the blastocyst stage. **Zygote**, *[S. l.]*, v. 22, n. 1, p. 69–79, 2012. DOI: 10.1017/S0967199412000299.

COMBELLES, Catherine M. H.; HOLICK, Emily A.; PAOLELLA, Louis J.; WALKER, David C.; WU, Qiaqia. Profiling of superoxide dismutase isoenzymes in compartments of the developing bovine antral follicles. **Reproduction**, *[S. l.]*, v. 139, n. 5, p. 871–881, 2010. DOI: 10.1530/REP-09-0390.

CORNET-BARTOLOMÉ, David; BARRAGÁN, Montserrat; ZAMBELLI, Filippo; FERRER-VAQUER, Anna; TISCORNIA, Gustavo; BALCELLS, Susanna; RODRIGUEZ, Amelia; GRINBERG, Daniel; VASSENA, Rita. Human oocyte meiotic maturation is associated with a specific profile of alternatively spliced transcript isoforms. **Molecular Reproduction and Development**, *[S. l.]*, v. 88, n. 9, p. 605–617, 2021. DOI: 10.1002/mrd.23526.

DA SILVEIRA, Juliano C. et al. Supplementation with small-extracellular vesicles from ovarian follicular fluid during in vitro production modulates bovine embryo development. **PLoS ONE**, *[S. l.]*, v. 12, n. 6, p. 1–25, 2017. DOI: 10.1371/journal.pone.0179451.

DA SILVEIRA, Juliano C.; VEERAMACHANENI, D. N. Ra.; WINGER, Quinton A.; CARNEVALE, Elaine M.; BOUMA, Gerrit J. Cell-secreted vesicles in equine ovarian follicular fluid contain mirnas and proteins: A possible new form of cell communication within the ovarian follicle. **Biology of Reproduction**, *[S. l.]*, v. 86, n. 3, p. 1–10, 2012. DOI: 10.1095/biolreprod.111.093252.

DA SILVEIRA, Juliano Coelho; ANDRADE, Gabriella Mamede; SIMAS, Rosineide Costa; MARTINS-JÚNIOR, Helio Alves; EBERLIN, Marcos Nogueira; SMITH, Lawrence Charles; PERECIN, Felipe; MEIRELLES, Flávio Vieira. Lipid profile of extracellular vesicles and their relationship with bovine oocyte developmental competence: New players in intra follicular cell communication. **Theriogenology**, *[S. l.]*, v. 174, p. 1–8, 2021. DOI: 10.1016/j.theriogenology.2021.07.024.

DE ÁVILA, ACFCM1 et al. Estrous cycle impacts miRNA content in extracellular vesicles that modulate bovine cumulus cell transcripts during in vitro maturation Running title: Effect of different estrous cycle on small EVs. **Biology of Reproduction**, *[S. l.]*, 2019.

DU, Chen; CHEN, Xiujuan. Transcriptome Profiling of Oocytes at the Germinal Vesicle Stage from Women from Mongolia with Polycystic Ovary Syndrome. **International Journal of General Medicine**, *[S. l.]*, v. Volume 14, p. 4469–4478, 2021. DOI: 10.2147/ijgm.s321853.

DUDA, Przemysław et al. Targeting GSK3 and Associated Signaling Pathways Involved in Cancer. **Cells**, *[S. l.]*, v. 9, n. 5, 2020. DOI: 10.3390/cells9051110.

FORTUNE, J. E. Ovarian Follicular Growth and Development in Mammals1. **Biology of Reproduction**, *[S. l.]*, v. 50, n. 2, p. 225–232, 1994. DOI: 10.1095/biolreprod50.2.225. Disponível em: https://doi.org/10.1095/biolreprod50.2.225.

GODAKUMARA, Kasun et al. Trophoblast derived extracellular vesicles specifically alter the transcriptome of endometrial cells and may constitute a critical component of embryo-maternal communication. **Reproductive Biology and Endocrinology**, *[S. l.]*, v. 19, n. 1, p. 1–14, 2021. DOI: 10.1186/s12958-021-00801-5.

GROSBOIS, J.; DEMEESTERE, I. Dynamics of PI3K and Hippo signaling pathways during in vitro human follicle activation. **Human Reproduction**, *[S. l.]*, v. 33, n. 9, p. 1705–1714, 2018. DOI: 10.1093/humrep/dey250.

HASAN, Mohammad Mehedi et al. Bovine follicular fluid and extracellular vesicles derived from follicular fluid alter the bovine oviductal epithelial cells transcriptome. **International Journal of Molecular Sciences**, *[S. l.]*, v. 21, n. 15, p. 1–16, 2020. DOI: 10.3390/ijms21155365.

HENG, Dai; WANG, Qiaozhi; MA, Xiaoshu; TIAN, Ye; XU, Kaili; WENG, Xuechun; HU, Xusong; LIU, Wenbo; ZHANG, Cheng. Role of OCT4 in the Regulation of FSH-Induced Granulosa Cells Growth in Female Mice. **Frontiers in Endocrinology**, *[S. l.]*, v. 10, n. January, p. 1–10, 2020. DOI: 10.3389/fendo.2019.00915.

HENNET, Margo L.; COMBELLES, Catherine M. H. The antral follicle: A microenvironment for oocyte differentiation. **International Journal of Developmental Biology**, *[S. l.]*, v. 56, n. 10–12, p. 819–831, 2012. DOI: 10.1387/ijdb.120133cc.

HERMIDA, Miguel A.; DINESH KUMAR, J.; LESLIE, Nick R. GSK3 and its interactions with the PI3K/AKT/mTOR signalling network. **Advances in Biological Regulation**, *[S. l.]*, v. 65, p. 5–15, 2017. DOI: 10.1016/j.jbior.2017.06.003. Disponível em: http://dx.doi.org/10.1016/j.jbior.2017.06.003.

HU, Junhe; TANG, Tao; ZENG, Zhi; WU, Juan; TAN, Xiansheng; YAN, Jiao. The expression of small RNAs in exosomes of follicular fluid altered in human polycystic ovarian syndrome. **PeerJ**, *[S. l.]*, v. 2020, n. 2, 2020. DOI: 10.7717/peerj.8640.

HUNG, Wei Ting; NAVAKANITWORAKUL, Raphatphorn; KHAN, Tarique; ZHANG, Pan; DAVIS, John S.; MCGINNIS, Lynda K.; CHRISTENSON, Lane K. Stage-specific follicular extracellular vesicle uptake and regulation of bovine granulosa cell proliferation. **Biology of Reproduction**, *[S. l.]*, v. 97, n. 4, p. 644–655, 2017. DOI: 10.1093/biolre/iox106.

JIAO, Yafei; ZHU, Shaoqian; LI, Jiaojiao; JAM ZAHEER, Ahmed; LI, Mengmei; HUANG, Ben. PS48 promotes in vitro maturation and developmental competence of porcine oocytes through activating PI3K/Akt signalling pathway. **Reproduction in Domestic Animals**, *[S. l.]*, v. 55, n. 12, p. 1678–1687, 2020. DOI: 10.1111/rda.13818.

JING, Hongyuan; CHEN, Yu; LIANG, Wan; CHEN, Miaoyu; QIU, Changwei; GUO, Meng yao. Effects of Selenium on MAC-T Cells in Bovine Mastitis: Transcriptome Analysis of Exosomal mRNA Interactions. **Biological Trace Element Research**, *[S. l.]*, v. 199, n. 8, p. 2904–2912, 2021. DOI: 10.1007/s12011-020-02439-7.

KAGEY, Michael H.; HE, Xi. Rationale for targeting the Wnt signalling modulator Dickkopf-1 for oncology. **British journal of pharmacology**, *[S. l.]*, v. 174, n. 24, p. 4637–4650, 2017.
KANEHISA, Minoru; GOTO, Susumu. KEGG: Kyoto Encyclopedia of Genes and Genomes. **Nucleic Acids Research**, *[S. l.]*, v. 28, n. 1, p. 27–30, 2000. DOI: 10.1093/nar/28.1.27. Disponível em: https://doi.org/10.1093/nar/28.1.27.

KANG, Woojin et al. Trehalose Suppresses Lysosomal Anomalies in Supporting Cells of Oocytes and Maintains Female Fertility. **Nutrients**, *[S. l.]*, v. 14, n. 10, 2022. DOI: 10.3390/nu14102156.

KIM, Dae Kyum et al. EVpedia: An integrated database of high-throughput data for systemic analyses of extracellular vesicles. **Journal of Extracellular Vesicles**, *[S. l.]*, v. 2, n. 1, 2013. DOI: 10.3402/jev.v2i0.20384.

KOWALCZYK, Alicja; WRZECIŃSKA, Marcjanna; CZERNIAWSKA-PIĄTKOWSKA, Ewa; KUPCZYŃSKI, Robert. Exosomes – Spectacular role in reproduction. **Biomedicine and Pharmacotherapy**, *[S. l.]*, v. 148, n. January, 2022. DOI: 10.1016/j.biopha.2022.112752.

KRISHER, Rebecca L. In vivo and in vitro environmental effects on mammalian oocyte quality. **Annual Review of Animal Biosciences**, *[S. l.]*, v. 1, p. 393–417, 2013. DOI: 10.1146/annurev-animal-031412-103647.

LEITÃO, Cintia Camurça Fernandes; BRITO, Ivina Rocha; FROTA, Isana Mara Aragão; SILVA, José Roberto Viana. Importância dos fatores de crescimento locais na regulação da foliculogênese ovariana em mamíferos. **Acta Scientiae Veterinariae**, *[S. l.]*, v. 37, n. 3, p. 215, 2009. DOI: 10.22456/1679-9216.16332.

LENTH R. emmeans: Estimated Marginal Means, aka Least-Squares Means. **R package version 1.8.8.**, 2023. Disponível em: https://CRAN.R-project.org/package=emmeans.

LIAO, Yang; SMYTH, Gordon K.; SHI, Wei. The R package Rsubread is easier, faster, cheaper and better for alignment and quantification of RNA sequencing reads. **Nucleic Acids Research**, *[S. l.]*, v. 47, n. 8, 2019. DOI: 10.1093/nar/gkz114.

LOBO, ROGERIO A.; DIZEREGA, GERE S.; MARRS, RICHARD P. Follicular Fluid Steroid Levels in Dysmature and Mature Follicles from Spontaneous and Hyperstimulated Cycles in Normal and Anovulatory Women*. **The Journal of Clinical Endocrinology & Metabolism**, *[S. l.]*, v. 60, n. 1, p. 81–87, 1985. DOI: 10.1210/jcem-60-1-81. Disponível em: https://doi.org/10.1210/jcem-60-1-81.

LONERGAN, P.; RIZOS, D.; GUTIERREZ-ADAN, A.; FAIR, T.; BOLAND, M. P. Oocyte and embryo quality: Effect of origin, culture conditions and gene expression patterns. **Reproduction in Domestic Animals**, *[S. l.]*, v. 38, n. 4, p. 259–267, 2003. DOI: 10.1046/j.1439-0531.2003.00437.x.

LOVE, Michael I.; HUBER, Wolfgang; ANDERS, Simon. Moderated estimation of fold change and dispersion for RNA-seq data with DESeq2. **Genome Biology**, *[S. l.]*, v. 15, n. 12, p. 1–21, 2014. DOI: 10.1186/s13059-014-0550-8.

MACAULAY, Angus D. et al. The gametic synapse: RNA transfer to the bovine oocyte. **Biology of Reproduction**, *[S. l.]*, v. 91, n. 4, p. 1–12, 2014. DOI: 10.1095/biolreprod.114.119867.

MACAULAY, Angus D. et al. Cumulus cell transcripts transit to the bovine oocyte in preparation for maturation. **Biology of Reproduction**, *[S. l.]*, v. 94, n. 1, p. 1–11, 2016. DOI: 10.1095/biolreprod.114.127571.

MACHTINGER, Ronit; BACCARELLI, Andrea A.; WU, Haotian. Extracellular vesicles and female reproduction. **Journal of Assisted Reproduction and Genetics**, *[S. l.]*, v. 38, n. 3, p. 549–557, 2021. DOI: 10.1007/s10815-020-02048-2.

MAKKER, Annu; GOEL, Madhu Mati; MAHDI, Abbas Ali. PI3K/PTEN/Akt and TSC/mTOR signaling pathways, ovarian dysfunction, and infertility: An update. **Journal of Molecular Endocrinology**, *[S. l.]*, v. 53, n. 3, p. R103–R118, 2014. DOI: 10.1530/JME-14-0220.

MARDONES, Muriel D.; ANDAUR, Gabriela A.; VARAS-GODOY, Manuel; HENRIQUEZ, Jenny F.; SALECH, Felipe; BEHRENS, María Isabel; COUVE, Andrés; INESTROSA, Nibaldo C.; VARELA-NALLAR, Lorena. Frizzled-1 receptor regulates adult hippocampal neurogenesis. **Molecular Brain**, *[S. l.]*, v. 9, n. 1, p. 29, 2016. DOI: 10.1186/s13041-016-0209-3. Disponível em: https://doi.org/10.1186/s13041-016-0209-3.

MARTÍNEZ-MORO, Álvaro; GONZÁLEZ-BRUSI, Leopoldo; LAMAS-TORANZO, Ismael; O'CALLAGHAN, Elena; ESTEVE-CODINA, Anna; LONERGAN, Pat; BERMEJO-ÁLVAREZ, Pablo. RNA-sequencing reveals genes linked with oocyte developmental potential in bovine cumulus cells. **Molecular Reproduction and Development**, *[S. l.]*, v. 89, n. 9, p. 399–412, 2022. DOI: https://doi.org/10.1002/mrd.23631. Disponível em: https://onlinelibrary.wiley.com/doi/abs/10.1002/mrd.23631.

MATHIVANAN, Suresh; FAHNER, Cassie J.; REID, Gavin E.; SIMPSON, Richard J. ExoCarta 2012: Database of exosomal proteins, RNA and lipids. **Nucleic Acids Research**, *[S. l.]*, v. 40, n. D1, p. 1241–1244, 2012. DOI: 10.1093/nar/gkr828.

MATOBA, Satoko; BENDER, Katrin; FAHEY, Alan G.; MAMO, Solomon; BRENNAN, Lorraine; LONERGAN, Patrick; FAIR, Trudee. Predictive value of bovine follicular components as markers of oocyte developmental potential. **Reproduction, Fertility and Development**, *[S. l.]*, v. 26, n. 2, p. 337–345, 2014. DOI: 10.1071/RD13007.

MATSUNO, Yuta; KANKE, Takuya; MARUYAMA, Natsumi; FUJII, Wataru; NAITO, Kunihiko; SUGIURA, Koji. Characterization of mRNA profiles of the exosome-like vesicles in porcine follicular fluid. **PLoS ONE**, *[S. l.]*, v. 14, n. 6, p. 1–16, 2019. DOI: 10.1371/journal.pone.0217760.

MENG, Lin; HU, Hongmei; LIU, Zhiqiang; ZHANG, Luyao; ZHUAN, Qingrui; LI, Xue; FU, Xiangwei; ZHU, Shien; HOU, Yunpeng. The Role of Ca2 + in Maturation and Reprogramming of Bovine Oocytes: A System Study of Low-Calcium Model. **Frontiers in Cell and Developmental Biology**, *[S. l.]*, v. 9, 2021. DOI: 10.3389/fcell.2021.746237. Disponível em: https://www.frontiersin.org/articles/10.3389/fcell.2021.746237.

MOTA, Gustavo Bruno. **Dissertação de Mestrado:** Desenvolvimento e expressão gênica em oócitos bovinos imaturos selecionados por azul cresil brilhante, 2008.

NAVAKANITWORAKUL, Raphatphorn; HUNG, Wei Ting; GUNEWARDENA, Sumedha; DAVIS, John S.; CHOTIGEAT, Wilaiwan; CHRISTENSON, Lane K. Characterization and small RNA content of extracellular vesicles in follicular fluid of developing bovine antral follicles. **Scientific Reports**, *[S. l.]*, v. 6, n. November 2015, p. 1–14, 2016. DOI: 10.1038/srep25486. Disponível em: http://dx.doi.org/10.1038/srep25486.

O'BRIEN, Killian; BREYNE, Koen; UGHETTO, Stefano; LAURENT, Louise C.; BREAKEFIELD, Xandra O. RNA delivery by extracellular vesicles in mammalian cells and its applications. **Nature Reviews Molecular Cell Biology**, *[S. l.]*, v. 21, n. 10, p. 585–606, 2020. DOI: 10.1038/s41580-020-0251-y. Disponível em: https://doi.org/10.1038/s41580-020-0251-y.

O'BRIEN, Yvonne; WINGFIELD, Mary; O'SHEA, Lynne C. Anti-Müllerian hormone and progesterone levels in human follicular fluid are predictors of embryonic development. **Reproductive Biology and Endocrinology**, *[S. l.]*, v. 17, n. 1, p. 1–8, 2019. DOI: 10.1186/s12958-019-0492-9.

PALMA, Gustavo Adolfo; ARGAÑARAZ, Martin Eduardo; BARRERA, Antonio Daniel; RODLER, Daniela; MUTTO, Adrian Ángel; SINOWATZ, Fred. Biology and biotechnology of follicle development. **The Scientific World Journal**, *[S. l.]*, v. 2012, n. Figure 1, 2012. DOI: 10.1100/2012/938138.

PAN, Yu; YANG, Sufang; CHENG, Juanru; LV, Qiao; XING, Qinghua; ZHANG, Ruimen; LIANG, Jingyuan; SHI, Deshun; DENG, Yanfei. Whole-Transcriptome Analysis of LncRNAs Mediated ceRNA Regulation in Granulosa Cells Isolated From Healthy and Atresia Follicles of Chinese Buffalo. **Frontiers in Veterinary Science**, *[S. l.]*, v. 8, n. July, p. 1–14, 2021. DOI: 10.3389/fvets.2021.680182.

READER, Karen L.; STANTON, Jo Ann L.; JUENGEL, Jennifer L. The role of oocyte organelles in determining developmental competence. **Biology**, *[S. l.]*, v. 6, n. 3, p. 1–22, 2017. DOI: 10.3390/biology6030035.

REGASSA, A.; RINGS, F.; HOELKER, M.; CINAR, U.; THOLEN, E.; LOOFT, C.; SCHELLANDER, K.; TESFAYE, D. Transcriptome dynamics and molecular cross-talk between bovine oocyte and its companion cumulus cells. **BMC Genomics**, *[S. l.]*, v. 12, 2011. DOI: 10.1186/1471-2164-12-57.

RODRIGUES, Thais A.; TUNA, Kubra M.; ALLI, Abdel A.; TRIBULO, P.; HANSEN, P. J.; KOH, Jin; PAULA-LOPES, F. F. Follicular fluid exosomes act on the bovine oocyte to improve oocyte competence to support development and survival to heat shock. **Reproduction, Fertility and Development**, *[S. l.]*, v. 31, n. 5, p. 888–897, 2019. DOI: 10.1071/RD18450.

R CORE TEAM. R: A Language and Environment for Statistical Computing. **R Foundation for Statistical Computing**, Vienna, Austria. 2023. Disponível em: https://www.R-project.org/.

SAMEREH, Sarah; HAJARIAN, Hadi; KARAMISHABANKAREH, Hamed; SOLTANI, Leila; FOROUTANIFAR, Saheb. Effects of different concentrations of Chir98014 as an activator of Wnt/beta-catenin signaling pathway on oocyte in-vitro maturation and subsequent embryonic development in Sanjabi ewes. **Reproduction in Domestic Animals**, *[S. l.]*, v. 56, n. 7, p. 965–971, 2021. DOI: 10.1111/rda.13938.

SAMPAIO, R. V. et al. Generation of bovine (Bos indicus) and buffalo (Bubalus bubalis) adipose tissue derived stem cells: Isolation, characterization, and multipotentiality. **Genetics and Molecular Research**, *[S. l.]*, v. 14, n. 1, p. 53–62, 2015. DOI: 10.4238/2015.January.15.7.
SANTOS, G. et al. Subclinical mastitis interferes with ovulation, oocyte and granulosa cell quality in dairy cows. **Theriogenology**, *[S. l.]*, v. 119, p. 214–219, 2018. DOI: 10.1016/j.theriogenology.2018.04.028.

SHORNING, Boris Y.; DASS, Manisha S.; SMALLEY, Matthew J.; PEARSON, Helen B. The PI3K-AKT-mTOR Pathway and Prostate Cancer: At the Crossroads of AR, MAPK, and WNT Signaling. **International Journal of Molecular Sciences**, *[S. l.]*, v. 21, n. 12, 2020. DOI: 10.3390/ijms21124507. Disponível em: https://www.mdpi.com/1422-0067/21/12/4507.

SIRARD, M. A.; DUFORT, I.; COENEN, K.; TREMBLAY, K.; MASSICOTTE, L.; ROBERT, C. The use of genomics and proteomics to understand oocyte and early embryo functions in farm animals. **Reproduction (Cambridge, England) Supplement**, *[S. l.]*, v. 61, p. 117–129, 2003. DOI: 10.1530/biosciprocs.5.010.

SIRARD, Marc André. Folliculogenesis and acquisition of oocyte competence in cows. **Animal Reproduction**, *[S. l.]*, v. 16, n. 3, p. 449–454, 2019. DOI: 10.21451/1984-3143-AR2019-0038.

SIRARD, Marc André; RICHARD, François; BLONDIN, Patrick; ROBERT, Claude. Contribution of the oocyte to embryo quality. **Theriogenology**, *[S. l.]*, v. 65, n. 1, p. 126–136, 2006. DOI: 10.1016/j.theriogenology.2005.09.020.

SKOG, Johan; WÜRDINGER, Tom; VAN RIJN, Sjoerd; MEIJER, Dimphna H.; GAINCHE, Laura; CURRY, William T.; CARTER, Bob S.; KRICHEVSKY, Anna M.; BREAKEFIELD, Xandra O. Glioblastoma microvesicles transport RNA and proteins that promote tumour growth and provide diagnostic biomarkers. **Nature Cell Biology**, *[S. l.]*, v. 10, n. 12, p. 1470–1476, 2008. DOI: 10.1038/ncb1800.

SOHEL, Md Mahmodul Hasan; HOELKER, Michael; SCHELLANDER, Karl; TESFAYE, Dawit. The extent of the abundance of exosomal and non-exosomal extracellular miRNAs in the bovine follicular fluid. **Reproduction in Domestic Animals**, *[S. l.]*, v. 57, n. 10, p. 1208–1217, 2022. DOI: 10.1111/rda.14195.

SPATE, Lee D.; BROWN, Alana N.; REDEL, Bethany K.; WHITWORTH, Kristin M.; MURPHY, Clifton N.; PRATHER, Randall S. Dickkopf-Related Protein 1 Inhibits the WNT Signaling Pathway and Improves Pig Oocyte Maturation. **PLoS ONE**, *[S. l.]*, v. 9, n. 4, p. e95114, 2014. DOI: 10.1371/journal.pone.0095114.

TAYLOR, Douglas D.; GERCEL-TAYLOR, Cicek. MicroRNA signatures of tumor-derived exosomes as diagnostic biomarkers of ovarian cancer. **Gynecologic Oncology**, *[S. l.]*, v. 110, n. 1, p. 13–21, 2008. DOI: 10.1016/j.ygyno.2008.04.033.

UZBEKOVA, Svetlana; ALMIÑANA, Carmen; LABAS, Valerie; TEIXEIRA-GOMES, Ana Paula; COMBES-SOIA, Lucie; TSIKIS, Guillaume; CARVALHO, Anais Vitorino; UZBEKOV, Rustem; SINGINA, Galina. Protein Cargo of Extracellular Vesicles From Bovine Follicular Fluid and Analysis of Their Origin From Different Ovarian Cells. **Frontiers in Veterinary Science**, *[S. l.]*, v. 7, n. November, 2020. DOI: 10.3389/fvets.2020.584948.

UZBEKOVA, Svetlana; SALHAB, Mohamad; PERREAU, Christine; MERMILLOD, Pascal; DUPONT, Joëlle. Glycogen synthase kinase 3B in bovine oocytes and granulosa cells: Possible involvement in meiosis during in vitro maturation. **Reproduction**, *[S. l.]*, v. 138, n. 2, p. 235–246, 2009. DOI: 10.1530/REP-09-0136.

VALADI, Hadi; EKSTRÖM, Karin; BOSSIOS, Apostolos; SJÖSTRAND, Margareta; LEE, James J.; LÖTVALL, Jan O. Exosome-mediated transfer of mRNAs and microRNAs is a novel mechanism of genetic exchange between cells. **Nature Cell Biology**, *[S. l.]*, v. 9, n. 6, p. 654–659, 2007. DOI: 10.1038/ncb1596.

VALVEZAN, Alexander; KLEIN, Peter. GSK-3 and Wnt Signaling in Neurogenesis and Bipolar Disorder. **Frontiers in Molecular Neuroscience**, *[S. l.]*, v. 5, 2012. DOI: 10.3389/fnmol.2012.00001. Disponível em: https://www.frontiersin.org/articles/10.3389/fnmol.2012.00001.

VEZIROGLU, Eren M.; MIAS, George I. Characterizing Extracellular Vesicles and Their Diverse RNA Contents. **Frontiers in Genetics**, *[S. l.]*, v. 11, n. July, p. 1–30, 2020. DOI: 10.3389/fgene.2020.00700.

WALKER, Bailey N.; BIASE, Fernando H. The blueprint of RNA storages relative to oocyte developmental competence in cattle (Bos taurus). **Biology of Reproduction**, *[S. l.]*, v. 102, n. 4, p. 784–794, 2020. DOI: 10.1093/biolre/ioaa015.

WALLACE, Martina; COTTELL, Evelyn; GIBNEY, Michael J.; MCAULIFFE, Fionnuala M.; WINGFIELD, Mary; BRENNAN, Lorraine. An investigation into the relationship between the metabolic profile of follicular fluid, oocyte developmental potential, and implantation outcome. **Fertility and Sterility**, *[S. l.]*, v. 97, n. 5, 2012. DOI: 10.1016/j.fertnstert.2012.01.122.

WANG, Liping; FAN, Hairui; ZOU, Yinggang; YUAN, Qiuyue; HU, Xuming; CHEN, Xujing; ZHU, Chunhui; ZHANG, Xiaomei; CUI, Hengmi. Aberrant Expression of Long Non-coding RNAs in Exosomes in Follicle Fluid From PCOS Patients. **Frontiers in Genetics**, *[S. l.]*, v. 11, n. February, p. 1–10, 2021. DOI: 10.3389/fgene.2020.608178.

YU, Guangchuang; WANG, Li Gen; HAN, Yanyan; HE, Qing Yu. ClusterProfiler: An R package for comparing biological themes among gene clusters. **OMICS A Journal of Integrative Biology**, *[S. l.]*, v. 16, n. 5, p. 284–287, 2012. DOI: 10.1089/omi.2011.0118.

ZENG, Bin; CHEN, Ting; XIE, Mei Ying; LUO, Jun Yi; HE, Jia Jian; XI, Qian Yun; SUN, Jia Jie; ZHANG, Yong Liang. Exploration of long noncoding RNA in bovine milk exosomes and their stability during digestion in vitro. **Journal of Dairy Science**, *[S. l.]*, v. 102, n. 8, p. 6726–6737, 2019. DOI: 10.3168/jds.2019-16257. Disponível em: http://dx.doi.org/10.3168/jds.2019-16257.

ZHANG, Yuan; LIU, Yunfeng; LIU, Haiying; TANG, Wai Ho. Exosomes: Biogenesis, biologic function and clinical potential. **Cell and Bioscience**, *[S. l.]*, v. 9, n. 1, p. 1–18, 2019. DOI: 10.1186/s13578-019-0282-2. Disponível em: https://doi.org/10.1186/s13578-019-0282-2.

ZHAO, Yahui; LUO, Aiping; LI, Sheng; ZHANG, Wei; CHEN, Hongyan; LI, Yi; DING, Fang; HUANG, Furong; LIU, Zhihua. Inhibitor of Differentiation/DNA Binding 1 (ID1) Inhibits Etoposide-induced Apoptosis in a c-Jun/c-Fos-dependent Manner*. **Journal of Biological Chemistry**, *[S. l.]*, v. 291, n. 13, p. 6831–6842, 2016. DOI: https://doi.org/10.1074/jbc.M115.704361. Disponível em: https://www.sciencedirect.com/science/article/pii/S0021925820429400.